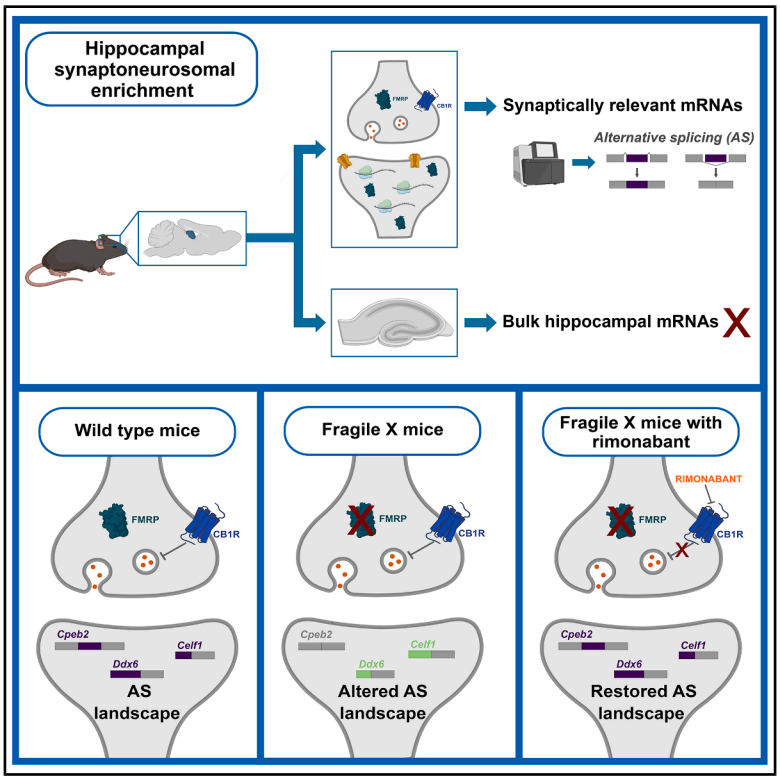
iScience

Article

CB1 receptor inhibition restores synaptoneurosomal alternative splicing landscape in fragile X syndrome mice

Graphical abstract



Highlights

- Synaptoneurosomes show an accurate representation of relevant synaptic mRNAs
- FMRP loss alters the hippocampal synaptic transcriptome related to RNA splicing
- AS landscape is modified in FX synaptoneurosomes in a treatment-dependent manner
- AS events reversed by rimonabant were validated in hippocampal synaptoneurosomes

Authors

Lucía de los Reyes-Ramírez, Laura Ciaran-Alfano, Marina Reixachs-Solé, ..., Rafael Maldonado, Eduardo Eyras, Andrés Ozaita

Correspondence

andres.ozaita@upf.edu

In brief

Biological sciences; Molecular neuroscience; Cognitive neuroscience

Reyes-Ramírez et al., 2026, iScience *29*, 117793
November 20, 2026 © 2026 The Authors. Published by Elsevier Inc.
https://doi.org/10.1016/j.isci.2026.117793

CellPress

iScience

CellPress
OPEN ACCESS

Article

CB1 receptor inhibition restores synaptoneurosomal alternative splicing landscape in fragile X syndrome mice

Lucía de los Reyes-Ramírez,[1,2] Laura Ciaran-Alfano,[1,2] Marina Reixachs-Solé,[3,4] Araceli Bergadà-Martínez,[2] Lorena Galera-López,[1,2] Sara Martínez-Torres,[2] Alba Navarro-Romero,[2] Rafael Maldonado,[2,5] Eduardo Eyras,[3,4] and Andrés Ozaita[1,2,6,*]

[1]Research Group in Biology of Cognition, Department of Medicine and Life Sciences, Universitat Pompeu Fabra, 08003 Barcelona, Spain
[2]Laboratory of Neuropharmacology-NeuroPhar, Department of Medicine and Life Sciences, Universitat Pompeu Fabra, 08003 Barcelona, Spain
[3]EMBL Australia Partner Laboratory Network at the Australian National University, Canberra, ACT 2601, Australia
[4]The John Curtin School of Medical Research, Canberra, ACT 2601, Australia
[5]Hospital Del Mar Medical Research Institute (IMIM), 08003 Barcelona, Spain
[6]Lead contact
*Correspondence: andres.ozaita@upf.edu
https://doi.org/10.1016/j.isci.2026.117793

SUMMARY

Fragile X syndrome (FXS), the most frequent heritable cause of intellectual disability and autism, involves impaired cognition and synaptic plasticity. Preclinical studies show that inhibition of the cannabinoid type-1 receptor (CB1R) restores key phenotypic traits in *Fmr1* knockout (FX) mice. However, the underlying molecular mechanisms remain undefined. We analyzed the hippocampal synaptoneurosomal transcriptome and confirmed that synaptoneurosomes are an accurate representation of synaptic composition and function. Then, we analyzed this transcriptome after pharmacological CB1R inhibition in male FX mice and found that rimonabant had limited impact at the gene expression level. Notably, detailed *in silico* analysis of alternative splicing (AS) revealed that rimonabant reverts numerous AS events in FX mice to wild-type levels. These changes in synaptoneurosomal AS landscape suggest a novel mechanism by which CB1R targeting may restore specific AS patterns. Altogether, our results reveal new molecular alterations in FXS context that are sensitive to pharmacological treatment related to cognitive alleviation.

INTRODUCTION

Fragile X syndrome (FXS) is the most prevalent inherited cause of intellectual disability and the most common monogenic cause of autism spectrum disorder (ASD) with an incidence of 1:4,000 males and 1:8,000 females.[1] It is caused by a trinucleotide CGG expansion in the 5′ untranslated region (5′ UTR) of the X-linked fragile X messenger ribonucleoprotein 1 gene (*FMR1*), which leads to *FMR1* hypermethylation and the subsequent loss of its related protein, FMRP.[2] FMRP is an RNA-binding protein (RBP) with a key role in local mRNA modulation in both pre- and postsynaptic compartments to maintain synaptic plasticity and connectivity.[3] FMRP also controls the activity of transcription factors, chromatin-modifying enzymes or RBPs key in RNA production and function.[4]

The *Fmr1* knockout (FX) mouse model[5] is the most widely used mouse model to study FXS. This model recapitulates some phenotypic traits of subjects with FXS, such as mild cognitive deficits, hyperactivity, or autistic-like behavior.[6] It also reproduces neuronal abnormalities including the alterations in density and morphology of dendritic spines,[7] dysregulation in the excitatory/inhibitory (E/I) balance[8] or the elevated group I mGluR5-dependent long-term depression (LTD) in the hippocampal CA1 region.[9] These processes are key for the correct establishment of synaptic homeostasis and plasticity, and their dysfunction can be the consequence of losing FMRP specifically at synaptic contacts. Given that synaptoneurosomes show an accurate representation of both pre- and postsynaptic parts of neuronal terminals and that FMRP is highly expressed at synapses, synaptoneurosomes may be used as an appropriate preparation to assess alterations in synaptic function.[10] In addition, the FXS model has allowed describing the impact of FMRP absence in the regulation of RNA alternative splicing (AS) in different brain regions and peripheral tissues.[11,12] Notably, alterations in AS are commonly observed in psychiatric and neurological disorders, including autism spectrum disorder,[13] although the specific alterations in FXS are largely unknown.

The endocannabinoid system (ECS) is an endogenous neuromodulatory network with a relevant role in cognition-associated processes.[14] Specifically, the cannabinoid type-1 receptor (CB1R), the main cannabinoid receptor of the ECS, can be pharmacologically or genetically inhibited to improve key phenotypes

This is an open access article under the CC BY-NC license (http://creativecommons.org/licenses/by-nc/4.0/).

in the FXS model. Indeed, it was previously described that both CB1R pharmacological inhibition and the genetic inhibition of CB1R, ameliorated cognitive deficits in FX mice.[15,16] In addition, low doses of rimonabant, a selective CB1R antagonist/inverse agonist, resolved the aberrant mGluR5-LTD, and the altered hippocampal spine density in FX mice.[15,16] Nevertheless, the molecular hallmarks underlying the behavioral and neurological improvements of rimonabant in FX mice remain unknown.

In the present study, we demonstrate that the use of hippocampal synaptoneurosomes allows performing a thorough assessment of synaptically relevant mRNAs. Furthermore, we reveal that in the hippocampal synaptic transcriptome of FX mice there is a complex modulation at the transcript level that can be modified by systemic CB1R inhibition. Interestingly, analysis of AS events revealed a significant set of changes in FX murine samples that were sensitive to CB1R inhibition with a very low dose of rimonabant. Altogether, the present study, by focusing on the synaptoneurosomal transcriptome, uncovers a previously unknown level of complexity in the effects of approaches that improve cognitive performance in FXS.

RESULTS

Synaptoneurosomes exhibit robust representation of the synaptic transcriptome

We used high-throughput RNA sequencing to identify gene populations in hippocampal synaptoneurosomes (HC-SYN) compared to bulk hippocampus (HC-BULK) to assess whether the synaptoneurosomal preparation improves the detection of synaptically relevant RNA species. Both types of RNA samples (HC-SYN and HC-BULK) were obtained from three wild-type (WT) mice starting from a single piece of hippocampal tissue that was split during sample processing to assess relative gene enrichment. We found a relevant effect of subcellular fractionation when comparing sample-to-sample variation in gene expression (Figure 1A), pointing to the type of subcellular fractionation (bulk hippocampus vs. synaptoneurosomes), instead of the mouse of origin, as the main characteristic influencing transcriptome identity. Differential gene expression (DGE) analysis comparing synaptoneurosomes and bulk hippocampus (HC-BULK vs. HC-SYN revealed 749 genes enriched in synaptoneurosomes while 1,019 genes were depleted in the same samples (Figure 1B; Table S1). Gene enrichment analysis showed that among the top-fifteen enriched Gene Ontology (GO) cellular component terms, most of them were related to synapses and transmembrane transport (Figure 1C). Moreover, among all enriched biological process GO terms, more than half of them (54%, 154/287) were associated with synaptic organization, synaptic plasticity, and mitochondrial activity, giving consistency to our strategy to study the synaptic transcriptome. Additionally, we analyzed synaptic processes and locations using the synaptic function annotation database *SynGO*. Specifically, we found that a relevant number of genes significantly enriched in synaptoneurosome samples compared to bulk hippocampus, were synapse-associated genes (Figure 1D). Thus, the study of synaptoneurosomes may provide a critical window into synaptic mechanisms driven by RNA modifications.

Sub-chronic CB1R inhibition with rimonabant shows the reversion in the expression of *Mff*, *Hnrnpd*, and *Slain2* in FX synaptoneurosomes

To determine molecular changes at synaptic contacts associated with the lack of FMRP and the effect that CB1R inhibition could have, we performed high-throughput RNA sequencing using synaptoneurosomes obtained from the hippocampus. By comparing FX and WT mice treated with vehicle (FX-VEH and WT-VEH, respectively), we found 29 genes upregulated and 19 genes downregulated (Figure 2A; Table S1). Out of these genes, we observed the upregulation of genes such as *Pcdhgb5* or *Gpr37* that were associated with dendritic arborization[17] and the ERK phosphorylation cascade,[18] respectively, and downregulation of *Fkbp5*, which has an effect on synaptic transmission[19] or *Rheb* that is implicated in mTORC1 signaling.[20]

Then, we analyzed the effect of sub-chronic systemic CB1R inhibition with rimonabant in FX and WT synaptoneurosomes. Rimonabant (0.1 mg/kg, 7 days) treatment modified the expression of 14 genes in FX synaptoneurosomes (Figure 2B; Table S1). Notably, in WT synaptoneurosomes, rimonabant uniquely upregulated *Col3a1* and *Cplan1* and downregulated *Pde2a*, none of them in common with the effect of rimonabant in FX samples (Figure S1A).

Next, to determine the specific effect of rimonabant in FX mice, we focused on those genes that were present in both comparisons (WT-VEH vs. FX-VEH and FX-VEH vs. FX-RIM) with an opposite expression: *Mff*, *Hnrnpd* and *Slain2* (Figures 2A and 2B). To further validate this reversion produced by rimonabant in FX mice, we assessed *Mff* and *Hnrnpd* mRNA expression levels in a different larger set of samples after rimonabant (0.1 mg/kg, 7 days) administration. RT-qPCR analysis in hippocampal synaptoneurosomes confirmed a decrease in the expression of *Mff* in FX mice that was reverted after sub-chronic treatment with rimonabant ($F(2,31) = 5.58$, $p = 0.008$; WT-VEH vs. FX-VEH $p = 0.008$; FX-VEH vs. FX-RIM $p = 0.04$) (Figure 2C) and a decrease in the expression of *Hnrnpd* mRNA levels in FX mice ($F(2,32) = 3.41$, $p = 0.04$; WT-VEH vs. FX-VEH $p = 0.04$) (Figure 2C). However, these changes were not present when bulk hippocampus homogenates were analyzed (Figure 2D), pointing to the relevance of studying synaptoneurosomal preparations to detect specific synaptically relevant changes in RNA expression.

Differential transcript expression analysis reveals a significant effect of CB1R inhibition in FX mice

Based on the results of *Hnrnpd*, a direct mRNA regulator,[21] and given that transcript expression allows for improved biological resolution and for decoding potentially important biological changes, we performed the DTE analysis with the same synaptoneurosomal transcriptomic datasets as mentioned above.

FX mice synaptoneurosomes showed 254 differentially expressed transcripts compared with WT mice synaptoneurosomes: 145 transcripts were upregulated in FX synaptoneurosomes while 109 were downregulated (Figure 3A; Table S2). Gene enrichment analysis of differentially expressed transcripts revealed an overrepresentation of synapse structure and synapse organization genes in both up and downregulated transcripts (Figures 3B and 3C), further validating the overrepresentation

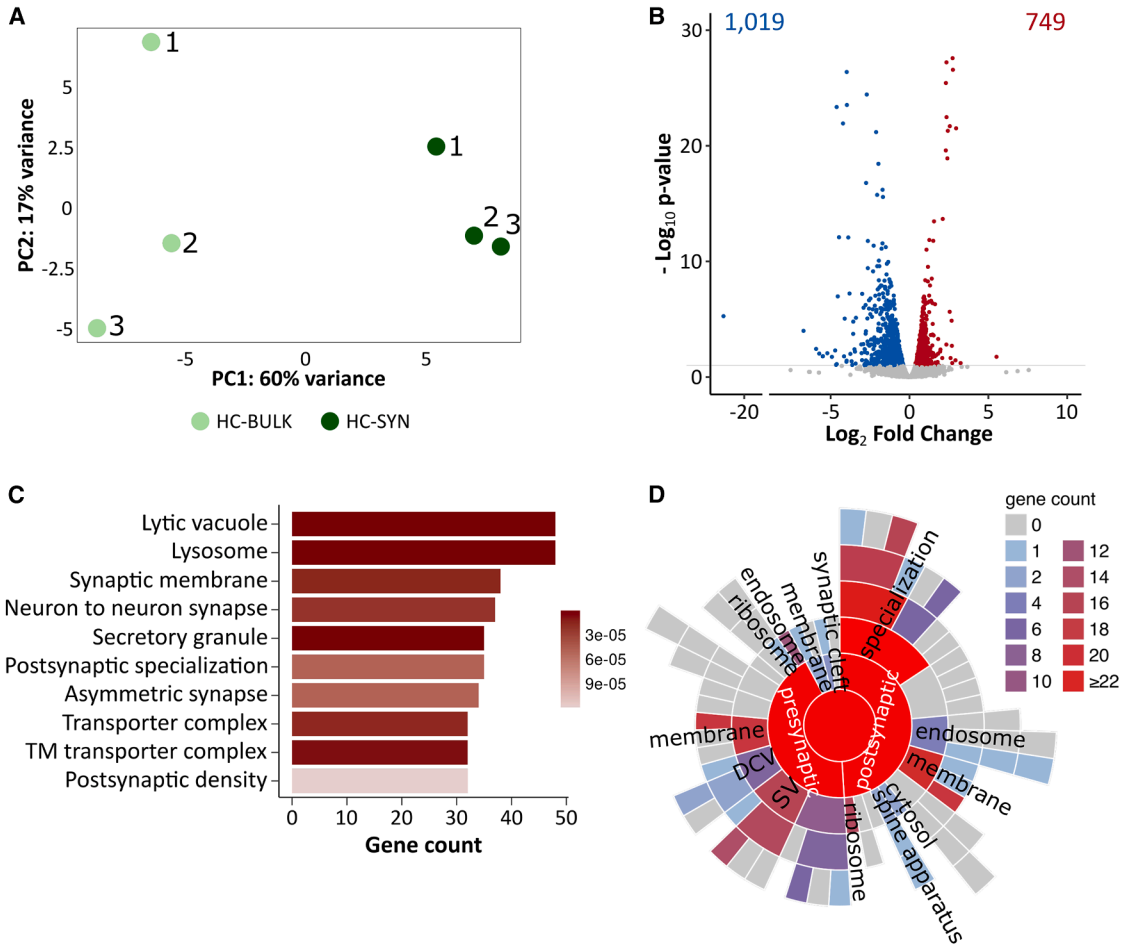


Figure 1. Transcriptomic profile of hippocampal synaptoneurosomes significantly differs from bulk hippocampal transcriptome

(A) Principal component analysis (PCA) of sequenced samples from the same animal, as denoted by numbers, colored based on sample type (HC-SYN, $n = 3$; HC-BULK, $n = 3$).

(B) Volcano plots of differentially expressed genes from hippocampal synaptoneurosome samples compared to bulk hippocampal samples (HC-BULK vs. HC-SYN). Blue dots represent 1,019 significantly depleted genes ($log_2FC < -0.2$ and adjusted p value < 0.1) and red dots 749 significantly enriched genes ($log_2FC > -0.2$ and adjusted p value < 0.1).

(C) Gene Ontology (GO) enrichment analysis for enriched genes in hippocampal synaptoneurosomes. GO terms represent only cellular components (CC).

(D) Sunburst plots of synaptic annotated ontologies for location (CC) terms. Colors are based on gene counts, including child terms. TM, transmembrane.

of synapse function using these synaptoneurosomal preparations. Among the downregulated transcripts, we also observed enrichment in biological processes associated with mRNA processing, such as regulation of mRNA metabolic process or RNA splicing (Figure 3B). Notably, within the 109 transcripts downregulated in FX synaptoneurosomes, we found some splicing factors such as *Celf2* or members of the *Hnrnp* family, pointing to a reduction in transcripts needed for mRNA processing and transcripts that may undergo splicing,[22] specifically at synaptic level.

We next analyzed the effect of rimonabant in FX mice at the transcript level. Differential transcript expression (DTE) comparing synaptoneurosomes from FX mice treated with rimonabant or vehicle showed 211 transcripts differentially expressed (Figure 3D; Table S2); specifically, 135 transcripts were upregulated while 76 were downregulated. Enrichment analysis of the associated genes only showed results among upregulated transcripts, which were related with synapse organization, mRNA splicing and neuron differentiation (Figure 3E). Interestingly, we found some transcripts from genes such as *Samd4b*, *Acin1*, or *Hnrnp* family (*Hnrnpa2b1*, *Hnrnpk*, and *Hnrnpd*) associated with mRNA metabolic processes and spliceosome function.

Then, we also assessed whether rimonabant administration had similar effects in WT mice. We observed 224 transcripts differentially expressed when we performed the DTE analysis (Figure S1B). Gene enrichment analysis showed no functional associations in terms of biological processes and few hits on molecular function and cellular component (Figure S1C), all very different from those functions observed in rimonabant-treated FX mice. These data further indicated that the effects of rimonabant at the synaptic transcriptomic level were genotype dependent.

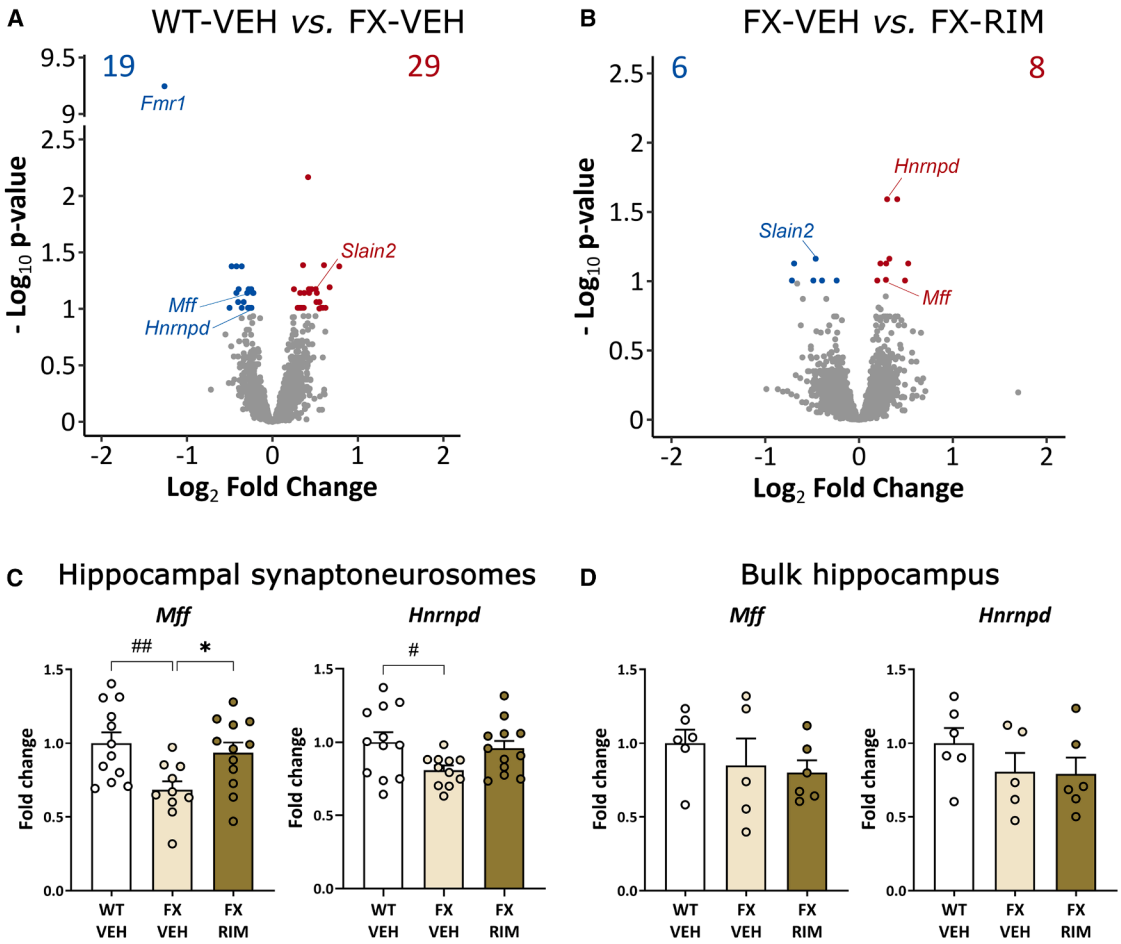


Figure 2. Systemic CB1R inhibition modulates the expression of *Mff* and *Hnrnpd* in FX hippocampal synaptoneurosomes

(A and B) Volcano plots of differentially expressed genes in (A) FX synaptoneurosomes compared with WT (WT-VEH vs. FX-VEH) and in (B) FX synaptoneurosomes treated with rimonabant (0.1 mg/kg, 7 days) or vehicle (FX-VEH vs. FX-RIM). Red and blue dots represent significantly up or downregulated genes, respectively. (WT-VEH, $n = 4$; FX-VEH, $n = 5$; FX-RIM, $n = 6$). Cut-off was set at $|\log_2 FC| > -0.2$ and adjusted p value < 0.1.

(C and D) Change in relative mRNA level of *Mff* and *Hnrnpd* from (C) hippocampal synaptoneurosomes and (D) bulk hippocampus measured by RT-qPCR. Data are expressed as mean ± SEM. #$p < 0.05$, ##$p < 0.01$ (genotype effect); *$p < 0.05$ (treatment effect) by one-way analysis of variance (ANOVA) with Tukey's post hoc test. (hippocampal synaptoneurosomes, $n = 10$–12; bulk hippocampus, $n = 5$–6).

As we did above with gene expression data, we assessed the specific effect of systemic CB1R inhibition in FX synaptoneurosomes by overlapping differentially expressed transcripts from both genotype and treatment comparisons. Out of all transcripts differentially expressed in FX synaptoneurosomes, 34% of them changed their expression in the opposite direction after rimonabant treatment (59 + 27 out of 254). Specifically, more than half of the downregulated transcripts in FX synaptoneurosomes (59 out of 109) were upregulated after rimonabant administration (hypergeometric test, $p = 1.8e^{-10}$) (Figure 4A; Table S2), while 27 upregulated transcripts in FX synaptoneurosomes were modulated in the opposite direction after treatment (Figure 4B; Table S2). Interestingly, while the 27 transcripts that were downregulated in FX synaptoneurosomes after CB1R inhibition were not enriched in any GO term, all the terms obtained in the gene enrichment analysis for the 59 transcripts modulated by rimonabant in FX synaptoneurosomes were related with mRNA processing and splicing (Figure 4C). This result reinforced the hypothesis that rimonabant treatment could ameliorate the synaptic alterations observed in FX mice by affecting mRNA splicing machinery.

FX synaptoneurosomes display a pattern of AS events that is sensitive to rimonabant administration

Given the implication of the differentially expressed transcripts in mRNA processing together with the described association between splicing and synaptic function,[13] the changes in the AS landscape were then investigated in synaptoneurosomes. We analyzed AS to obtain direct evidence in terms of skipping exon (SE), alternative first and last exon (AF and AL), alternative 5′ and 3′ splice-site (A5 and A3), mutually exclusive exons (MX), and retained intron (RI) (Figure S2A). The lack of *Fmr1* in hippocampal synaptoneurosomes dysregulated the splicing pattern of 206 genes by direct modification of 259 AS events (Figure 5A; Figure S3; Table S3). AF and SE were by far the

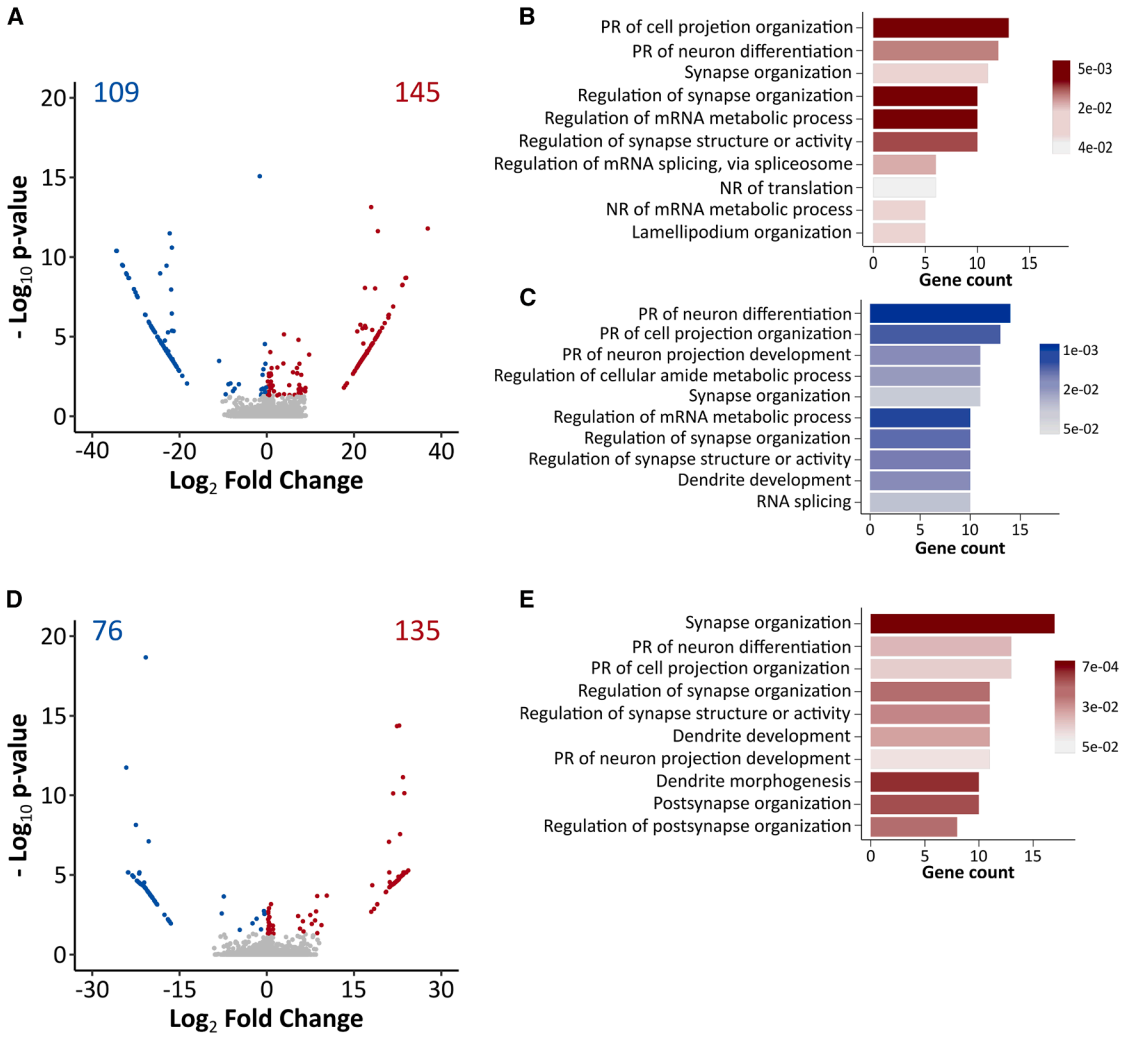


Figure 3. Transcriptomic landscape of FX hippocampal synaptoneurosomes at transcript level after vehicle or rimonabant administration

(A) Volcano plots of differentially expressed transcripts in (A) FX compared to WT (WT-VEH vs. FX-VEH). Red and blue dots represent significantly up or downregulated genes, respectively.

(B and C) Bar plots showing the top 10 most representative GO terms associated with up- (B) and downregulated (C) transcripts in FX synaptoneurosomes. GO terms represent only biological processes (BP).

(D) Volcano plots of differentially expressed transcripts in FX synaptoneurosomes treated with rimonabant (0.1 mg/kg, 7 days) (RIM) compared with those treated with vehicle (FX-VEH vs. FX-RIM).

(E) Bar plots showing the top 10 most representative GO terms from biological processes associated with upregulated transcripts in FX-treated mice. For volcanos, cut-off was set at $|\log_2 FC| > -0.2$ and adjusted p value < 0.05 (WT-VEH, $n = 4$; FX-VEH, $n = 5$; FX-RIM, $n = 6$). For the GO enrichment plots, terms were ordered by the number of genes related with the process and the gradient color is proportional to the significance.

most prevalent categories. While only 20% of the genes that we detected to present AS were also described to undergo splicing in hippocampal slices from FX mice (Figure S4),[11] this is the first time that changes in AS were detected specifically in FX synaptoneurosomes. Among the alternatively spliced events between FX and WT mice, we found genes associated with synaptic transmission and synaptic morphology such as *Cpeb2*, *FosB*, *Arf4*, *Cacng5*, or *Vdac3*.

We next analyzed AS events in rimonabant-treated FX synaptoneurosomes. This revealed the modification of 178 splicing events in 130 genes compared to non-treated FX synaptoneurosomes (Figure 5B; Figure S3; Table S3). Although fewer events seemed to be regulated by rimonabant, the most representative types of events were again AF and SE. Interestingly, among these events, we found transcripts encoding for ion channels and enzymes that could play a role in gene expression regulation and synaptic transmission such as *Gprin1*, *Kcnip4*, *Gabra5*, *Celf1*, *Mecp2*, *Hnmt*, or *Arc*.

To pinpoint the modifications driven by systemic CB1R inhibition, we compared splicing events in synaptoneurosomes from FX-treated mice with those FX and WT mice treated with vehicle. When we overlapped both sets of AS events, 77 events out of 56

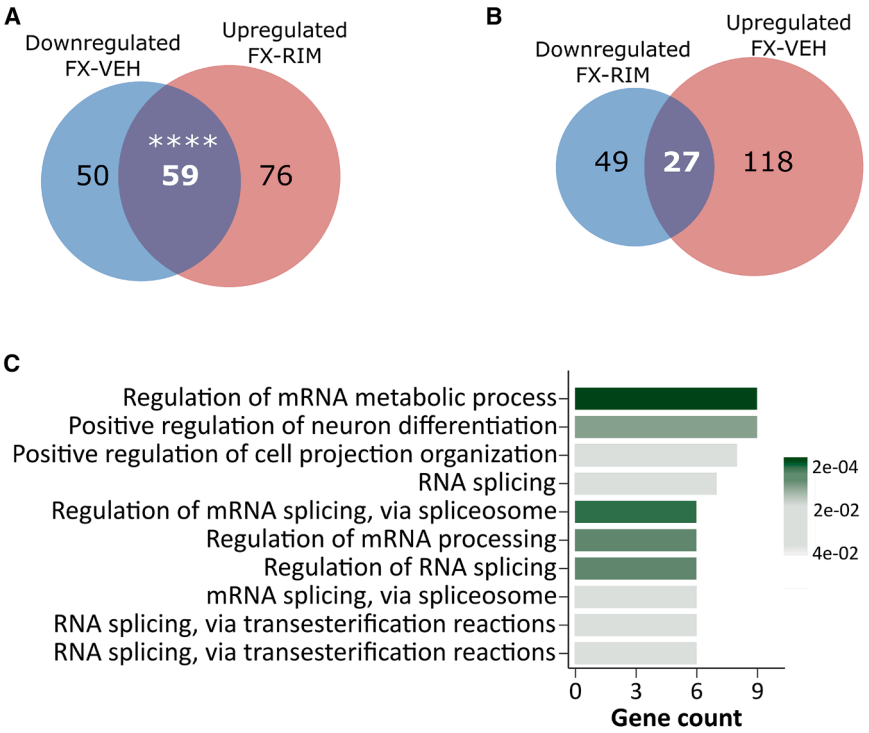


Figure 4. Sub-chronic systemic CB1R inhibition modulates altered transcript expression in FX and WT hippocampal synaptoneurosomes

(A and B) Venn diagrams of transcripts that were (A) downregulated in FX (WT-VEH vs. FX-VEH) and upregulated after rimonabant (0.1 mg/kg, 7 days) treatment (FX-VEH vs. FX-RIM) and (B) upregulated in FX (WT-VEH vs. FX-VEH) and downregulated after rimonabant treatment (FX-VEH vs. FX-RIM).

(C) Bar plots showing the top 10 most representative biological processes associated with genes from downregulated transcripts in FX synaptoneurosomes that were upregulated in FX synaptoneurosomes after rimonabant administration. ****$p < 0.0001$, by hypergeometric test. GO terms were ordered by the number of genes and the gradient color is proportional to the significance.

genes were common between genotype and treatment comparisons (Figure 5C). Again, only around 30% of the genes that presented AS events and that are sensitive to CB1R inhibition were previously described to be alternatively spliced in FX bulk hippocampal preparations.[11] To further analyze this low overlap, we cross-referenced the expression of these genes within a murine hippocampal transcriptomic single-cell dataset.[23] We found 46 out of 56 genes within the dataset, and from those, around 67% are predominantly expressed in neurons, with a significant subset showing exclusive neuronal specific (Figure S5). Specifically, these events occur in genes associated with RNA processing (*Celf1*, *Ddx6*, and *Rbm39*), cytoskeleton modulation (*Slain2*, *Nek3*, and *Tpm4*), ion channels (*Gprin1, Lrrcd8*), neuronal development (*Psap, Rims3*), and mitochondrial processes (*Atp5pb*), among others. Moreover, we observed a significant negative correlation between the direction and the magnitude of the change in significant events, mainly occurring in RBPs, in both FX synaptoneurosomes treated with rimonabant and vehicle (R Pearson = -0.97, $p < 2.2e^{-16}$) (Figure 5C). Interestingly, most of the events that were sensitive to CB1R inhibition in FX mice were not significantly modified after rimonabant administration in WT mice. Indeed, some interesting events selected for further validation were only significantly detected in FX synaptoneurosomes after vehicle or rimonabant treatment (WT-VEH vs. FX-VEH and FX-VEH vs. FX-RIM) and not in WT synaptoneurosomes after rimonabant administration (WT-VEH vs. WT-RIM) (Figure 5D), indicating the specific modulation of these AS events in FX synaptoneurosomes. Thus, a significant proportion of the AS events in FX mice could be rescued by systemic CB1R inhibition with a low dose of rimonabant in a genetic context-specific manner.

Inclusion and exclusion splicing events detected *in silico* were validated with specific probes

To further confirm the opposite modulation of these 77 AS events, we prioritize them based on functional relevance, transcript abundance, and the magnitude of the reversion of those that were previously described as brain-specific RBPs[24] (Figure S6). Thus, we validated the RBPs *Ddx6*, *Celf1*, and *Cpeb2* using newly generated tissue samples and customized TaqMan assays (Figures S2B and S7) with a substantially larger sample size. This approach allowed the measurement of changes both in the complete AS event but also in each transcript isoform resulting from AS. Transcripts covering the A5 event in *Ddx6*, an RNA helicase associated with translation suppression and mRNA degradation[25] presented similar results when we measured transcripts that cover event inclusion and exclusion. *Ddx6* exon inclusion was downregulated in FX synaptoneurosomes and upregulated after rimonabant administration in FX mice ($F(2,33) = 6.46$, $p = 0.004$; WT-VEH vs. FX-VEH $p = 0.01$; FX-VEH vs. FX-RIM $p = 0.006$) (Figure 6A), and the same modulation was observed in *Ddx6* exon exclusion ($F(2,33) = 7.95$, $p = 0.001$; WT-VEH vs. FX-VEH $p = 0.005$; FX-VEH vs. FX-RIM $p = 0.003$) (Figure 6B). The exclusion of this A5 event in FX mice resulted in a shorter 5′ UTR, however the inclusion may transcribe an isoform with a longer 5′ UTR or a non-translatable protein. In the case of AF event in *Celf1*, an RBP involved in post-translational modifications,[26] transcripts that cover both exon inclusion ($F(2,34) = 8.46$, $p = 0.001$; Tukey, WT-VEH vs. FX-VEH $p = 0.03$) (Figure 6C) and exon exclusion ($F(2,33) = 8.05$, $p = 0.001$; FX-VEH vs. FX-RIM $p = 0.0009$) (Figure 6D) were significantly more abundant in FX mice after rimonabant treatment, although only exon inclusion was also decreased in FX vehicle-treated mice ($F(2,34) = 8.46$, $p = 0.001$; FX-VEH vs. FX-RIM $p = 0.0007$) (Figure 6C). To note, the inclusion of this AF exon introduces a regulatory sequence in the promoter that favors the translation of a shorter N-terminal protein in the case of WT mice and rimonabant-treated FX mice. Lastly, we

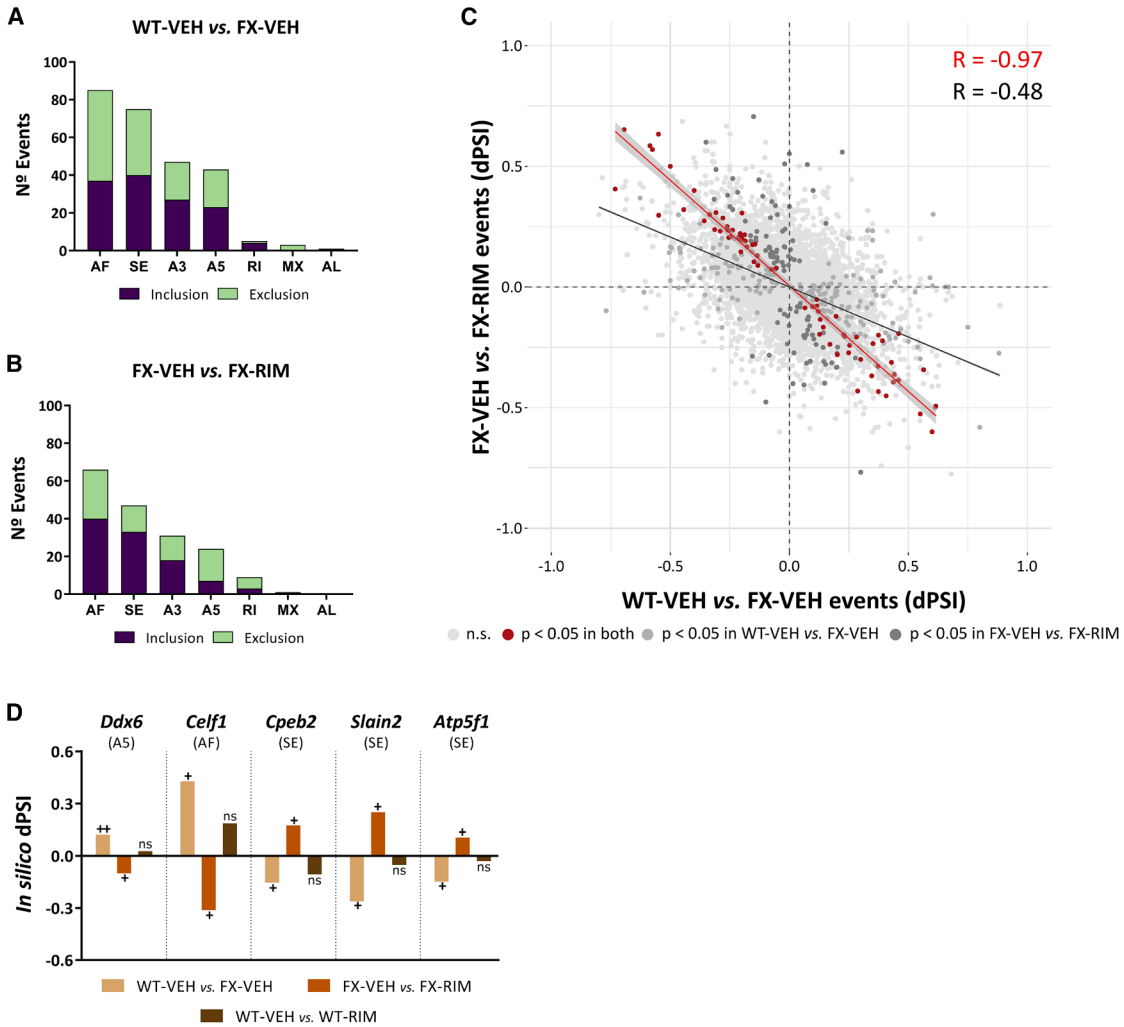


Figure 5. Sub-chronic systemic CB1R inhibition changes the direction of AS events in FX hippocampal synaptoneurosomes

(A and B) Histogram of AS types identified in (A) FX compared with WT and in (B) FX treated and non-treated with rimonabant (0.1 mg/kg, 7 days) (RIM). SE, skipping exon; MX, mutually exclusive exons; A5 and A3, alternative 5′ and 3′ splice-site, respectively; RI, retained intron; AF and AL, alternative first and last exon, respectively.

(C) Correlation plot of splicing events identified in both comparisons. In red, significant events in both comparisons (77); in gray and dark gray, significant events only in WT-VEH vs. FX-VEH (182) or FX-VEH vs. FX-RIM (101) comparisons, respectively. Red line shows the correlation of the red points and gray line the correlation of all other events detected in at least one comparison. Significant events were established based on a |dPSI| > 0.05 and false discovery rate (FDR) < 0.05.

(D) dPSI values of selected AS events that significantly revert their expression after rimonabant (0.1 mg/kg) (RIM) administration in FX but not in WT mice. Data are expressed as dPSI. ns, not significant; $+p < 0.05$, $++p < 0.01$ (in each comparison) by linear regression model following FDR correction (WT-VEH, $n = 4$; WT-RIM, $n = 5$; FX-VEH, $n = 5$; FX-RIM, $n = 6$).

also tested an SE event described in *Cpeb2*, another RBP that may regulate synaptic plasticity.[27,28] We found that exon inclusion was less present in FX synaptoneurosomes compared to WT ($F(2,34) = 5.67$, $p = 0.007$; WT-VEH vs. FX-VEH $p = 0.01$) (Figure 6E) and exon exclusion showed a non-significant tendency to be also less expressed in FX mice ($F(2,33) = 3.23$, $p = 0.051$) (Figure 6F). In addition, exon inclusion was also more present in rimonabant-treated FX mice compared with vehicle-treated FX mice ($F(2,34) = 5.67$, $p = 0.007$; FX-VEH vs. FX-RIM $p = 0.02$) (Figure 6E). In this AS event, inclusion or exclusion of a 90-bp exon produces two different functional isoforms that are described to differentially regulate RNA translation.[29] Remarkably, these transcript isoforms were not modified in bulk hippocampus homogenates from FX mice neither after vehicle nor after rimonabant treatment (Figure S8), reinforcing the relevance of synaptoneurosomal preparations in the study of specific transcript variations.

Finally, we calculated an experimental differential percent spliced in (dPSI) to measure whether the complete AS event was modified as it was each specific isoform. We found that *Cpeb2* SE event changed in HC-SYN in the same direction as *in silico* dPSI: negative in WT-VEH vs. FX-VEH and positive in

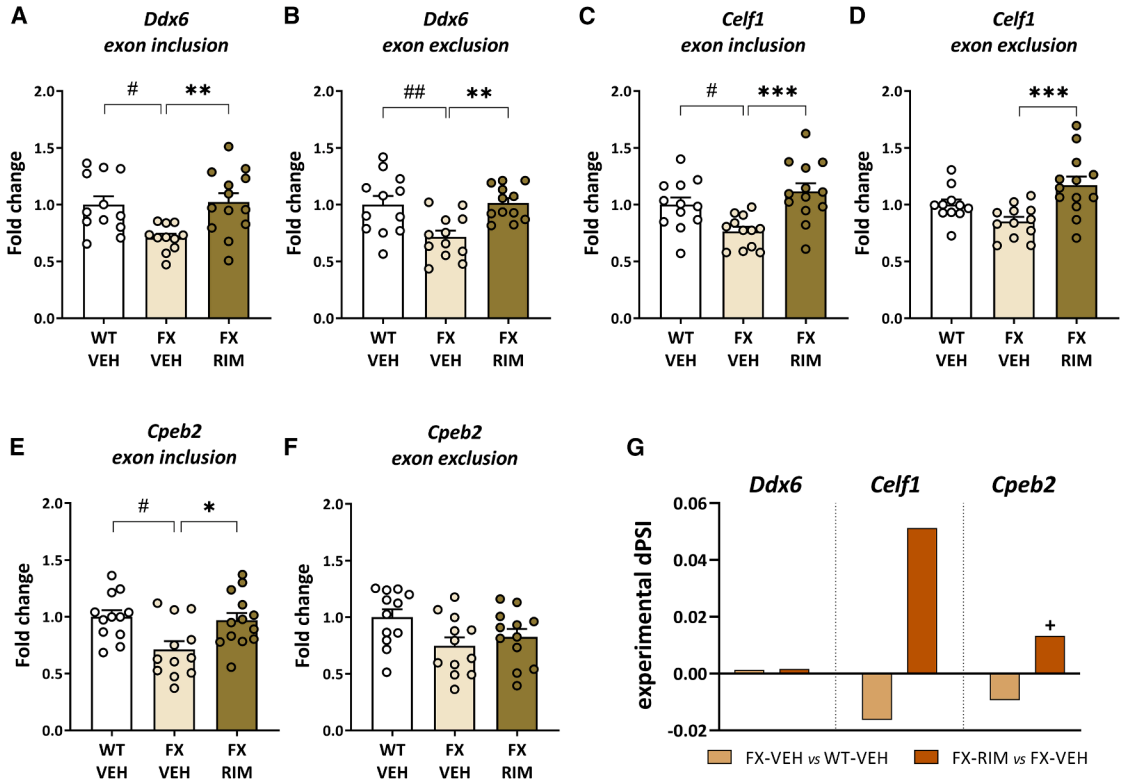


Figure 6. AS event-associated transcripts were modified in FX hippocampal synaptoneurosomes after sub-chronic systemic CB1R inhibition

(A–F) Hippocampal synaptoneurosome transcripts that defined (A) *Ddx6* inclusion, (B) *Ddx6* exclusion, (C) *Celf1* inclusion, (D) *Celf1* exclusion, (E) *Cpeb2* inclusion, and (F) *Cpeb2* exclusion were quantified referred to *18S* endogenous control. Data are expressed as mean ± SEM. #$p < 0.05$, ##$p < 0.01$ (genotype effect); *$p < 0.05$, **$p < 0.01$, and ***$p < 0.001$ (treatment effect) by one-way ANOVA with Tukey's post hoc test.

(G) Experimental calculation of the differences in PSI (experimental dPSI) in each comparison (WT-VEH vs. FX-VEH and FX-VEH vs. FX-RIM). Data are expressed as mean of experimental dPSI. +$p < 0.05$ (in each comparison) by Student's *t* test (n = 11–13).

FX-VEH vs. FX-RIM (Student's *t* test, $p = 0.01$) (Figure 6G); while the other two AS events did not reach significance. Moreover, the *Ddx6* A5 event also changed in the same direction as *in silico* in bulk hippocampal homogenates from rimonabant-treated FX mice (Student's *t* test, $p < 0.001$) (Figure S8G). Altogether, while we fully validated individual transcript isoforms associated with these three AS events in hippocampal synaptoneurosomes, only *Cpeb2* complete AS event was confirmed as significantly modulated in our independent validation cohort. Therefore, we showed that AS changes observed by high-throughput assessment in FX hippocampal synaptoneurosomes, can also be detected through complementary approaches in a different set of samples. This allowed the detection of specific AS events associated with FXS and their pharmacological modulation.

DISCUSSION

We used synaptoneurosomal transcriptomics to study the impact of *Fmr1* genetic ablation, the cause of FXS, on synaptically relevant mRNA, and the result of exposing FX mice to a treatment inhibiting CB1R. Thus, we analyzed the synaptic transcriptome of FX and WT male littermates after 7 days of rimonabant (or vehicle) administration, since this treatment schedule improves cognitive performance and synaptic plasticity in the FXS model.[16] We detected few changes in the overall DGE when WT and FX samples were compared. Instead, when potential transcripts were independently considered, the analysis revealed a decreased expression of mRNAs involved in synapse organization and RNA processing due to the genetic mutation. Interestingly, detailed study of synaptic AS events further demonstrated specific changes associated with the mutation that were reversed by the pharmacological inhibition of CB1R. The present study provides evidence for characteristic RNA splicing events in adult FX hippocampal synapses that are sensitive to CB1R pharmacological inhibition.

Synapses are highly specialized cellular structures that interconnect neurons and allow intercellular communication. The co-isolation of pre- and post-synaptic structures emerges as a useful technique to understand key molecular mechanisms underlying synaptic plasticity. Indeed, the solid evidence of mRNA presence and local protein synthesis at synaptic level[30,31] allows for both transcriptomic and proteomic approaches to unraveling the molecular mechanisms governing synaptic function. We previously characterized our preparation of synaptoneurosomes at proteomic level[32] and now we have also explored its content on synaptic mRNA species. To assure

proper comparison, the study of the synaptic mRNA enrichment was performed using the same piece of tissue and initial homogenate to render both synaptic and bulk RNA preparations. We found a major benefit of analyzing synaptic transcriptomes is that low abundant mRNAs are enriched. Indeed, among the enriched genes in hippocampal synaptoneurosomes compared to bulk hippocampus, we found genes linked to synapse architecture, synaptic plasticity, and, interestingly, many genes connected to mitochondrial bioenergetics. This agrees with previous studies showing that murine synaptoneurosomes were enriched in transcripts associated not only with synaptic density and ion transport mRNAs but also with energy metabolism- and mitochondria-related mRNAs.[33] In addition, both synapse organization and mitochondrial function play essential roles in hippocampal-dependent memory.[34] Indeed, synapses are the cellular compartment with the highest energy consumption,[35] as they maintain local protein synthesis, calcium homeostasis, cytoskeletal dynamics, neurotransmitter release and membrane modifications, and trafficking.[36]

The use of synaptoneurosomes to understand synaptic processes has become particularly relevant for the evaluation of neuronal changes and altered signaling pathways in neurological disorders, including FXS.[37] Since FMRP is localized both pre- and postsynaptically,[38] where it interacts with mRNAs and regulates mRNA translation synapses,[4] unraveling the impact of its loss at synapses is crucial. So far, transcriptomic studies in FXS were focused on the analysis of specific FMRP targets[39–41] or on ribosome profiling[11,42] rather than assessing total RNA expression. Therefore, synaptoneurosomal mRNA analysis, rather than bulk preparations, could identify synaptic pathways dysregulated in FXS and sensitive to pharmacological interventions.

Previous studies in our group have pointed to the inhibition of CB1R to improve memory performance in FX mice.[15,16] Specifically, low doses of the systemic CB1R antagonist/inverse agonist, rimonabant, or the neutral CB1R antagonist NESS0327, or even the hemideletion of the CB1R gene, improved several key features of FX mice including those associated with synaptic structure and plasticity.[15,16] To understand the synaptic alterations in FX mice as well as the impact of therapeutic intervention directed to CB1R, we analyzed synaptoneurosomes from rimonabant-treated and vehicle-treated FX and WT mice. We paid special attention to those modifications in which changes occurred in opposite directions when studying FX synaptoneurosomes after rimonabant or vehicle treatment.

We observed a downregulation of *Mff* mRNA expression in FX that was normalized to WT levels with rimonabant treatment, which is in accordance with previous findings about FMRP regulation of MFF translation[43] and with CB1R-mediated changes of mitochondrial dynamics.[44] Our results in murine FX synaptoneurosomes also showed downregulation in *Hnrnpd*. This gene encodes for heterogeneous nuclear ribonucleoprotein D, HNRNP D, also known as AUF1, a well-characterized RBP with a role in synapse formation and plasticity,[45,46] and described as FMRP target in HEK293 cells.[39] Interestingly, the dysfunction of HNRNP proteins was previously associated with neurological disorders, including fragile X tremor ataxia.[22] Moreover, studies in rat primary neuronal cultures reported an increase in HNRNP proteins at synapses, proposing that these proteins can regulate dendritic spine morphology.[47] Thus, the decrease that we observed in *Hnrnpd* expression could be associated with the elevated immature spines observed in FX mice that were significantly reduced after sub-chronic rimonabant treatment.[15] The reduction in the expression of HNRNP D was also associated with a dysregulation in the stability of mRNAs,[48] which could suggest a possible relation between FMRP and HNRNP D: in the absence of FMRP, dysregulated mRNA translation could lead to altered synaptic function.[49] Our findings let us hypothesize that the downregulation in *Hnrnpd* expression in FX mice could contribute to the dysregulation in the degradation of the excessive mRNAs that are synthesized in the absence of FMRP.

Gene expression changes in *Mff* and *Hnrnpd* were uniquely validated in hippocampal synaptoneurosomes and not in bulk hippocampal homogenates obtained from the same animals. This finding strongly suggests that the molecular regulation reflects local mRNA trafficking and activity-dependent translation occurring directly at the synapse.[30] Since changes in synaptic compartments can be diluted when analyzing bulk homogenates, the use of subcellular enrichment such as synaptoneurosomes is essential to accurately capture molecular alterations underlying synaptic function. Moreover, this issue is particularly critical in the case of FXS, in which FMRP acts primarily as a translational repressor of mRNAs within synaptic contacts.[50]

Gene expression is a complex process in which pre-mRNA splicing and RNA metabolism control the abundance and the location of expressed proteins, and in which HNRNP D has a key role.[21] Based on this, we further analyzed changes in transcript expression in FX hippocampal synaptoneurosomes since DTE analysis considers the different versions of transcripts that can be encoded by a single gene. DTE showed a greater number of hits compared to that at gene level, meaning that in FX mice, changes in RNA biology could critically contribute to the phenotypic alterations and the therapeutic effect of CB1R inhibition. In the FX synaptic transcriptome, we found up and downregulated transcripts associated with synapse structure and organization. This agrees with previous research in which the lack of FMRP has revealed an aberrant expression of relevant genes associated with brain development and structural plasticity.[51] Moreover, when focusing only on downregulated transcripts, we observed an enrichment in mRNA metabolic processes and RNA splicing. Interestingly, after rimonabant treatment, transcripts associated with mRNA regulation and spliceosome appeared among the upregulated ones in FX synaptoneurosomes. Given that alterations that affect the epigenetic landscape, including RNA metabolism and AS[52] could be associated with cognitive impairment,[53] we hypothesized that the cognitive alleviation observed after CB1R inhibition with rimonabant[15,16] could be associated with changes in the splicing machinery.

The analysis of the AS landscape showed major modifications. Indeed, 28 out of 206 genes (~14%) that undergo splicing in FX synaptoneurosomes are described as FMRP targets according to previous studies in bulk tissues.[40,41] Based on AS modifications, many studies show that splicing is modulated in subjects with ASD[54,55] and in central and peripheral tissues of FX mice,[11,12] although few of those genes previously described were in common with our results. This subtle overlap may imply

that most of these novel AS events in FX mice are highly localized to synaptic compartments and were therefore previously undetectable in bulk homogenates, further reinforcing the use of synaptoneurosomes as a tool to better understand synaptic functions.

Notably, some of our observed AS changes were sensitive to CB1R inhibition with a low dose of rimonabant, which strongly supports the existence of a regulatory mechanism where the ECS actively modulates the synaptic machinery of AS in agreement with CB1R modulation of key learning and memory mRNAs.[56] Of note, we found that *Slain2* was alternatively spliced between treated and non-treated FX mice, and its mRNA levels were also sensitive to rimonabant administration in FX mice. This dual regulation may also support a multilevel impact of CB1R signaling that extends beyond gene and transcript abundance to include post-transcriptional processing. In addition, the CB1R-sensitive changes in AS of *Atp5pb*, could be associated with the elevated mitochondrial leak found in FX mice[57] and with the observed dysregulation of *Mff*.

Notably, a relevant number of the genes that were alternatively spliced in FX synaptoneurosomes in a rimonabant-dependent manner were RBPs, which included those that were further validated (*Ddx6*, *Celf1*, and *Cpeb2*). *Cpeb2* AS event was validated in a different cohort of hippocampal synaptoneurosomes, but not in bulk hippocampus homogenates, reinforcing the use of synaptoneurosomal to study synaptic mRNAs. Instead, *Ddx6* and *Celf1* AS events were not validated in the additional synaptoneurosomal samples, which may be explained by technical and biological variability. Regarding technical variability, RT-qPCR has lower resolution and inherent noise compared to high-throughput RNA sequencing. Although gene and transcript expression were robustly validated in larger independent cohorts, RT-qPCR-based experimental dPSI calculations for AS events suffer from reduced statistical power. Regarding biological variability, *Ddx6* inclusion would produce a longer 5′ UTR or a non-translated isoform, while the two potential isoforms of *Celf1*, although having different functional impacts on translation efficiency, are produced at similar expression levels,[58] making difficult their specific detection by RT-qPCR.

Nevertheless, based on the genes that bear AS events in FX mice, it is unlikely that FMRP is a direct regulator of splicing. Instead, it can mediate RNA processing by regulating other downstream RBPs that ultimately regulate key processes for synaptic transmission. This is supported by the fact that a relevant number of the reverted AS events in our study occurred in RBPs, including brain-specific RBPs[24] that were selected for validation. Therefore, CB1R inhibition, through RBP modulation, may influence key downstream cascades that are dysregulated in FX mice. For instance, the AS event in *Celf1* contributes to the generation of two isoforms that differ in the presence of a regulatory sequence in the 5′ UTR and the N-terminal length.[59] The inclusion of this regulatory sequence is significantly increased in synaptoneurosomes from WT and rimonabant-treated FX mice, indicating a potential role in modulating translation efficiency. Such differential inclusion in *Celf1*, sensitive to rimonabant, provides a potential mechanistic link between treatment-sensitive AS regulation in FX mice and translation control that will deserve further research. Similarly, the AS of *Cpeb2* suggests a similar rescue of translation. Specifically, the inclusion isoform is linked to translation activation and the exclusion to translation repression,[60] although this specific isoform regulation has not been studied on neurons. Given that *Cpeb2* controls the translation of neuron-specific mRNAs essential for the maintenance of synaptic plasticity,[61,62] we hypothesize that increased translation of these target mRNAs in FX synaptoneurosomes results in excessive local protein synthesis, which may underlie the synaptic deficits and cognitive impairment observed in FX mice. In this regard, another CPEB protein has been previously described to impair E/I balance in a model of FXS by excessive translation of AMPAR subunits.[63] Finally, the reversion into *Cpeb2* exclusion after CB1R inhibition in FX mice could result in the attenuation of protein synthesis and the restoration of synaptic plasticity.

Thus, by restoring specific AS patterns of synaptic RBPs like *Celf1* and *Cpeb2*, CB1R inhibition may trigger a cascade that normalizes the synaptic microenvironment. This molecular rescue may also be aligned with the described association between other RBP isoforms like *Rbfox1* and changes in E/I balance,[64] a common neurobiological feature of ASD and FXS.[8,65] Since synapse function and formation respond to neuronal activity, the AS of these RBPs could be somehow associated with the further transcription and translation of key proteins to maintain an E/I balance. Consequently, the normalization of these AS-altered patterns provides a novel and compartment-specific mechanistic basis for the observed therapeutic potential of CB1R inhibition in FX mice, suggesting that AS of key RBPs and synaptic mRNAs is a critical step in the alleviation of phenotypic traits. Further studies will determine whether these RNA changes by rimonabant translate to specific protein isoforms rescuing FXS synaptic physiology.

Together, loss of FMRP results in changes in expression patterns in hippocampal synaptoneurosomes, which are most apparent when transcripts are independently analyzed and AS events are considered. As most of the genes that were alternatively spliced in FX synaptoneurosomes sensitive to rimonabant intervention were RBPs, we propose that these genes may play an intermediate role in the translation of genes directly associated with synaptic modifications. Altogether, our results suggest that the inhibition of CB1R in the FXS context modifies synaptic mRNA splicing of specific RBPs which could be related to the phenotypic improvement previously demonstrated by such pharmacological intervention.

Limitations of the study

A few limitations must be taken into consideration while evaluating the results of this study. Firstly, we characterized at the transcriptomic level the synaptoneurosomal fractions to study synaptic RNAs. This enriched fraction could include fractions of other cell types apart from pre- and postsynaptic neuronal components. Although neurons were the cells most frequently harboring the genes identified, we cannot rule out that the AS modification could happen in other cell types. Then, further investigation will be critical to uncover whether our findings are specific of rimonabant treatment or depend on specific CB1R inhibition at the synapses. Rimonabant is a systemic CB1R antagonist/inverse agonist that was withdrawn from the

market and can only be used experimentally. However, our results were obtained with a very low dose, previously reported to alleviate FXS phenotypic traits.[16] Thus, although rimonabant at high doses could have some side effects in specific populations,[66] in this study, we demonstrate that this very low dose modified FX mice synaptic transcriptome without altering WT transcriptome. Finally, while *in silico* detection of AS changes clearly demonstrated the reversion in the direction of many AS events, we observed more subtle changes when validated in a different set of samples. It is possible that these AS events were more efficiently detected by high-throughput sequencing where millions of reads cover the event rather than with TaqMan probes, in which the number of molecules detectable is lower. It also remains unclear whether the magnitude of these AS events can vary between individuals or whether could differ between cell types. We identified changes in AS events in hippocampal synaptoneurosomes that were sensitive to rimonabant treatment, but further studies need to be done to establish the connection between synaptic AS changes and the improvement of FXS phenotypic traits and to assess possible sex-related differences as only male FX mice were used. It should be noted that AS studies in subjects with FXS are currently very limited, even in peripheral tissues. Finally, to address the differences between mice and humans, AS changes may be assessed in "post-mortem" samples or in neurons derived from subjects with FXS to further confirm the translational relevance of our findings.

RESOURCE AVAILABILITY

Lead contact

Requests for further information and resources should be directed to and will be fulfilled by the lead contact, Andrés Ozaita (andres.ozaita@upf.edu).

Materials availability

This study did not generate new unique reagents.

Data and code availability

- RNA-seq raw data were deposited into the Gene Expression Omnibus (GEO) database under accession number GSE284627 for hippocampal synaptoneurosomes and bulk hippocampus from the same animal and GSE285032 for WT and FX hippocampal synaptoneurosomes treated with vehicle or rimonabant (0.1 mg/kg, 7 days).
- This paper does not report original code.
- Any additional information required to reanalyze the data reported in this paper is available from the lead contact upon reasoned request.

ACKNOWLEDGMENTS

We are grateful to Raquel Martín, Dulce Real, and Francisco Porrón for expert technical assistance and the Genomics Core Facility (MELIS-UPF) and the Scientific Computing Core Facility (MELIS-UPF) for helpful discussion and support. L.R.-R. was supported by a predoctoral fellowship from the Spanish Ministry of Science and Innovation (PRE2019-087644). L.C.-A. was supported by a predoctoral fellowship from the Spanish Ministry of Science and Innovation (PRE2022-101774). A.B.-M. was supported by predoctoral fellowship from Spanish Ministry of Universities (FPU20/02061). L.G.-L. was supported by a FRAXA Research Foundation postdoctoral fellowship. This work was supported by the Spanish Ministry of Science and Innovation (PID2021-123482OB-I00) and the La Marató de TV3 Foundation (202224-30-31) to A.O.; FRAXA Research Foundation (04-3222167) to L.G.-L. and A.O.; and Generalitat de Catalunya, AGAUR (2021 SGR 00912) to R.M.

AUTHOR CONTRIBUTIONS

Conceptualization, L.R.-R., M.R.-S., E.E., and A.O.; data curation, L.R.-R. and E.E.; formal analysis, L.R.-R., L.C.-A., and M.R.-S.; investigation, L.R.-R., L.C.-A., M.R.-S., A.B.-M., L.G.-L., S.M.-T., A.N.-R., E.E., and A.O.; methodology, L.R.-R., L.C.-A., M.R.-S., A.B.-M., L.G.-L., S.M.-T., A.N.-R., E.E., and A.O.; validation, L.R.-R. and A.B.-M.; visualization, L.R.-R., L.C.-A., and M.R.-S.; funding acquisition, R.M., E.E., and A.O.; resources, R.M., E.E., and A.O.; supervision, E.E. and A.O.; project administration, A.O.; writing – original draft, L.R.-R. and A.O.; writing – review and editing, L.R.-R., L.C.-A., M.R.-S., A.B.-M., L.G.-L., S.M.-T., A.N.-R., R.M., E.E., and A.O.

DECLARATION OF INTERESTS

R.M. and A.O. declare intellectual property of the patent PCT/EP2013/055728.

STAR★METHODS

Detailed methods are provided in the online version of this paper and include the following:

- KEY RESOURCES TABLE
- EXPERIMENTAL MODEL AND STUDY PARTICIPANT DETAILS
- METHOD DETAILS
  - Drugs
  - Hippocampal bulk and synaptoneurosomal preparation from mouse brain
  - Synaptoneurosomal enrichment preparation
  - RNA extraction
  - RNA sequencing analysis
  - Differential expression analysis
  - Alternative splicing analysis
  - Cell-type specificity enrichment analysis
  - Specific assays for alternative splicing events
  - Gene expression and alternative splicing analysis by qRT-PCR
- QUANTIFICATION AND STATISTICAL ANALYSIS

SUPPLEMENTAL INFORMATION

Supplemental information can be found online at https://doi.org/10.1016/j.isci.2026.117793.

Received: February 2, 2026
Revised: May 13, 2026
Accepted: September 21, 2026

REFERENCES

1. Hagerman, R.J., Berry-Kravis, E., Hazlett, H.C., Bailey, D.B., Moine, H., Kooy, R.F., Tassone, F., Gantois, I., Sonenberg, N., Mandel, J.L., and Hagerman, P.J. (2017). Fragile X syndrome. Nat. Rev. Dis. Primers *3*, 17065. https://doi.org/10.1038/nrdp.2017.65.
2. Verkerk, A.J.M.H., Pieretti, M., Sutcliffe, J.S., Fu, Y.H., Kuhl, D.P.A., Pizzuti, A., Reiner, O., Richards, S., Victoria, M.F., Zhang, F., et al. (1991). Identification of a gene (FMR-1) containing a CGG repeat coincident with a breakpoint cluster region exhibiting length variation in fragile X syndrome. Cell *65*, 905–914. https://doi.org/10.1016/0092-8674(91)90397-H.
3. Sidorov, M.S., Auerbach, B.D., and Bear, M.F. (2013). Fragile X mental retardation protein and synaptic plasticity. Mol. Brain *6*, 15. https://doi.org/10.1186/1756-6606-6-15.
4. Richter, J.D., and Zhao, X. (2021). The molecular biology of FMRP: new insights into fragile X syndrome. Nat. Rev. Neurosci. *22*, 209–222. https://doi.org/10.1038/s41583-021-00432-0.
5. The, D.-B.F.X.C., Bakker, C.E., Verheij, C., Willemsen, R., van der Helm, R., Oerlemans, F., Vermey, M., Bygrave, A., Hoogeveen, A.T., Oostra,

B.A., et al. (1994). Fmr1 knockout mice: A model to study fragile X mental retardation. Cell *78*, 23–33. https://doi.org/10.1016/0092-8674(94)90569-X.

6. Salcedo-Arellano, M.J., Dufour, B., McLennan, Y., Martinez-Cerdeno, V., and Hagerman, R. (2020). Fragile X syndrome and associated disorders: Clinical aspects and pathology. Neurobiol. Dis. *136*, 104740. https://doi.org/10.1016/J.NBD.2020.104740.
7. Jawaid, S., Kidd, G.J., Wang, J., Swetlik, C., Dutta, R., and Trapp, B.D. (2018). Alterations in CA1 hippocampal synapses in a mouse model of fragile X syndrome. Glia *66*, 789–800. https://doi.org/10.1002/GLIA.23284.
8. Contractor, A., Klyachko, V.A., and Portera-Cailliau, C. (2015). Altered neuronal and circuit excitability in Fragile X Syndrome. Neuron *87*, 699–715. https://doi.org/10.1016/J.NEURON.2015.06.017.
9. Bear, M.F., Huber, K.M., and Warren, S.T. (2004). The mGluR theory of fragile X mental retardation. Trends Neurosci. *27*, 370–377. https://doi.org/10.1016/J.TINS.2004.04.009.
10. Rubeis, S.D., and Bagni, C. (2009). Synaptosome. Encyclopedia of Neuroscience, 3982–3985. https://doi.org/10.1007/978-3-540-29678-2_5831.
11. Shah, S., Molinaro, G., Liu, B., Wang, R., Huber, K.M., and Richter, J.D. (2020). FMRP Control of Ribosome Translocation Promotes Chromatin Modifications and Alternative Splicing of Neuronal Genes Linked to Autism. Cell Rep. *30*, 4459–4472.e6. https://doi.org/10.1016/j.celrep.2020.02.076.
12. Jung, S., Shah, S., Han, G., and Richter, J.D. (2023). FMRP deficiency leads to multifactorial dysregulation of splicing and mislocalization of MBNL1 to the cytoplasm. PLoS Biol. *21*, e3002417. https://doi.org/10.1371/JOURNAL.PBIO.3002417.
13. Gandal, M.J., Zhang, P., Hadjimichael, E., Walker, R.L., Chen, C., Liu, S., Won, H., Van Bakel, H., Varghese, M., Wang, Y., et al. (2018). Transcriptome-wide isoform-level dysregulation in ASD, schizophrenia, and bipolar disorder. Science *362*, eaat8127. https://doi.org/10.1126/SCIENCE.AAT8127.
14. Zou, S., and Kumar, U. (2018). Cannabinoid Receptors and the Endocannabinoid System: Signaling and Function in the Central Nervous System. Int. J. Mol. Sci. *19*, 833. https://doi.org/10.3390/IJMS19030833.
15. Busquets-Garcia, A., Gomis-González, M., Guegan, T., Agustín-Pavón, C., Pastor, A., Mato, S., Pérez-Samartín, A., Matute, C., de la Torre, R., Dierssen, M., et al. (2013). Targeting the endocannabinoid system in the treatment of fragile X syndrome. Nat. Med. *19*, 603–607. https://doi.org/10.1038/nm.3127.
16. Gomis-González, M., Busquets-Garcia, A., Matute, C., Maldonado, R., Mato, S., and Ozaita, A. (2016). Possible Therapeutic Doses of Cannabinoid Type 1 Receptor Antagonist Reverses Key Alterations in Fragile X Syndrome Mouse Model. Genes *7*, 56. https://doi.org/10.3390/GENES7090056.
17. Li, Y., Xiao, H., Chiou, T.T., Jin, H., Bonhomme, B., Miralles, C.P., Pinal, N., Ali, R., Chen, W.V., Maniatis, T., and De Blas, A.L. (2012). Molecular and Functional Interaction between Protocadherin-γC5 and GABAA Receptors. J. Neurosci. *32*, 11780–11797. https://doi.org/10.1523/JNEUROSCI.0969-12.2012.
18. Meyer, R.C., Giddens, M.M., Schaefer, S.A., and Hall, R.A. (2013). GPR37 and GPR37L1 are receptors for the neuroprotective and glioprotective factors prosaptide and prosaposin. Proc. Natl. Acad. Sci. USA *110*, 9529–9534. https://doi.org/10.1073/PNAS.1219004110.
19. Qiu, B., Xu, Y., Wang, J., Liu, M., Dou, L., Deng, R., Wang, C., Williams, K.E., Stewart, R.B., Xie, Z., et al. (2019). Loss of FKBP5 Affects Neuron Synaptic Plasticity: An Electrophysiology Insight. Neuroscience *402*, 23–36. https://doi.org/10.1016/j.neuroscience.2019.01.021.
20. Zou, J., Zhou, L., Du, X.X., Ji, Y., Xu, J., Tian, J., Jiang, W., Zou, Y., Yu, S., Gan, L., et al. (2011). Rheb1 Is Required for mTORC1 and Myelination in Postnatal Brain Development. Dev. Cell *20*, 97–108. https://doi.org/10.1016/j.devcel.2010.11.020.
21. Yoon, J.H., De, S., Srikantan, S., Abdelmohsen, K., Grammatikakis, I., Kim, J., Kim, K.M., Noh, J.H., White, E.J.F., Martindale, J.L., et al. (2014). PAR-CLIP analysis uncovers AUF1 impact on target RNA fate and genome integrity. Nat. Commun. *5*, 5248. https://doi.org/10.1038/ncomms6248.
22. Low, Y.H., Asi, Y., Foti, S.C., and Lashley, T. (2021). Heterogeneous Nuclear Ribonucleoproteins: Implications in Neurological Diseases. Mol. Neurobiol. *58*, 631–646. https://doi.org/10.1007/S12035-020-02137-4.
23. Yao, Z., van Velthoven, C.T.J., Nguyen, T.N., Goldy, J., Sedeno-Cortes, A.E., Baftizadeh, F., Bertagnolli, D., Casper, T., Chiang, M., Crichton, K., et al. (2021). A taxonomy of transcriptomic cell types across the isocortex and hippocampal formation. Cell *184*, 3222–3241.e26. https://doi.org/10.1016/J.CELL.2021.04.021.
24. Perez-Perri, J.I., Ferring-Appel, D., Huppertz, I., Schwarzl, T., Sahadevan, S., Stein, F., Rettel, M., Galy, B., and Hentze, M.W. (2023). The RNA-binding protein landscapes differ between mammalian organs and cultured cells. Nat. Commun. *14*, 2074. https://doi.org/10.1038/s41467-023-37494-w.
25. Di Stefano, B., Luo, E.C., Haggerty, C., Aigner, S., Charlton, J., Brumbaugh, J., Ji, F., Rabano Jiménez, I., Clowers, K.J., Huebner, A.J., et al. (2019). The RNA Helicase DDX6 Controls Cellular Plasticity by Modulating P-Body Homeostasis. Cell Stem Cell *25*, 622–638.e13. https://doi.org/10.1016/J.STEM.2019.08.018.
26. Lambert, N., Robertson, A., Jangi, M., McGeary, S., Sharp, P.A., and Burge, C.B. (2014). RNA Bind-n-Seq: quantitative assessment of the sequence and structural binding specificity of RNA binding proteins. Mol. Cell *54*, 887–900. https://doi.org/10.1016/J.MOLCEL.2014.04.016.
27. Ivshina, M., Lasko, P., and Richter, J.D. (2014). Cytoplasmic polyadenylation element binding proteins in development, health, and disease. Annu. Rev. Cell Dev. Biol. *30*, 393–415. https://doi.org/10.1146/ANNUREV-CELLBIO-101011-155831.
28. Wu, L., Wells, D., Tay, J., Mendis, D., Abbott, M.A., Barnitt, A., Quinlan, E., Heynen, A., Fallon, J.R., and Richter, J.D. (1998). CPEB-mediated cytoplasmic polyadenylation and the regulation of experience-dependent translation of alpha-CaMKII mRNA at synapses. Neuron *21*, 1129–1139. https://doi.org/10.1016/S0896-6273(00)80630-3.
29. Turimella, S.L., Bedner, P., Skubal, M., Vangoor, V.R., Kaczmarczyk, L., Karl, K., Zoidl, G., Gieselmann, V., Seifert, G., Steinhäuser, C., et al. (2015). Characterization of cytoplasmic polyadenylation element binding 2 protein expression and its RNA binding activity. Hippocampus *25*, 630–642. https://doi.org/10.1002/HIPO.22399.
30. Hafner, A.S., Donlin-Asp, P.G., Leitch, B., Herzog, E., and Schuman, E.M. (2019). Local protein synthesis is a ubiquitous feature of neuronal pre- And postsynaptic compartments. Science *364*, eaau3644. https://doi.org/10.1126/science.aau3644.
31. Cajigas, I.J., Tushev, G., Will, T.J., Tom Dieck, S., Fuerst, N., and Schuman, E.M. (2012). The Local Transcriptome in the Synaptic Neuropil Revealed by Deep Sequencing and High-Resolution Imaging. Neuron *74*, 453–466. https://doi.org/10.1016/j.neuron.2012.02.036.
32. Salgado-Mendialdúa, V., Aguirre-Plans, J., Guney, E., Reig-Viader, R., Maldonado, R., Ozaita, A., Bayés, À., and Oliva, B. (2018). Δ9-tetrahydrocannabinol modulates the proteasome system in the brain. Biochem. Pharmacol. *157*, 159–168. https://doi.org/10.1016/J.BCP.2018.08.026.
33. Simbriger, K., Amorim, I.S., Chalkiadaki, K., Lach, G., Jafarnejad, S.M., Khoutorsky, A., and Gkogkas, C.G. (2020). Monitoring translation in synaptic fractions using a ribosome profiling strategy. J. Neurosci. Methods *329*, 108456. https://doi.org/10.1016/J.JNEUMETH.2019.108456.
34. Underwood, E.L., Redell, J.B., Hood, K.N., Maynard, M.E., Hylin, M., Waxham, M.N., Zhao, J., Moore, A.N., and Dash, P.K. (2023). Enhanced presynaptic mitochondrial energy production is required for memory formation. Sci. Rep. *13*, 14431. https://doi.org/10.1038/S41598-023-40877-0.
35. Faria-Pereira, A., and Morais, V.A. (2022). Synapses: The Brain's Energy-Demanding Sites. Int. J. Mol. Sci. *23*, 3627. https://doi.org/10.3390/IJMS23073627.

36. Rodríguez-Berdini, L., and Caputto, B.L. (2019). Lipid Metabolism in Neurons: A Brief Story of a Novel c-Fos-Dependent Mechanism for the Regulation of Their Synthesis. Front. Cell. Neurosci. *13*, 198. https://doi.org/10.3389/FNCEL.2019.00198.

37. Wang, Y.Z., and Savas, J.N. (2018). Uncovering Discrete Synaptic Proteomes to Understand Neurological Disorders. Proteomes *6*, 30. https://doi.org/10.3390/PROTEOMES6030030.

38. Antar, L.N., Afroz, R., Dictenberg, J.B., Carroll, R.C., and Bassell, G.J. (2004). Metabotropic Glutamate Receptor Activation Regulates Fragile X Mental Retardation Protein and Fmr1 mRNA Localization Differentially in Dendrites and at Synapses. J. Neurosci. *24*, 2648–2655. https://doi.org/10.1523/JNEUROSCI.0099-04.2004.

39. Ascano, M., Mukherjee, N., Bandaru, P., Miller, J.B., Nusbaum, J.D., Corcoran, D.L., Langlois, C., Munschauer, M., Dewell, S., Hafner, M., et al. (2012). FMRP targets distinct mRNA sequence elements to regulate protein expression. Nature *492*, 382–386. https://doi.org/10.1038/NATURE11737.

40. Darnell, J.C., Van Driesche, S.J., Zhang, C., Hung, K.Y.S., Mele, A., Fraser, C.E., Stone, E.F., Chen, C., Fak, J.J., Chi, S.W., et al. (2011). FMRP stalls ribosomal translocation on mRNAs linked to synaptic function and autism. Cell *146*, 247–261. https://doi.org/10.1016/j.cell.2011.06.013.

41. Maurin, T., Lebrigand, K., Castagnola, S., Paquet, A., Jarjat, M., Popa, A., Grossi, M., Rage, F., and Bardoni, B. (2018). HITS-CLIP in various brain areas reveals new targets and new modalities of RNA binding by fragile X mental retardation protein. Nucleic Acids Res. *46*, 6344–6355. https://doi.org/10.1093/NAR/GKY267.

42. Das Sharma, S., Metz, J.B., Li, H., Hobson, B.D., Hornstein, N., Sulzer, D., Tang, G., and Sims, P.A. (2019). Widespread Alterations in Translation Elongation in the Brain of Juvenile Fmr1 Knockout Mice. Cell Rep. *26*, 3313–3322.e5. https://doi.org/10.1016/J.CELREP.2019.02.086.

43. Fenton, A.R., Peng, R., Bond, C., Hugelier, S., Lakadamyali, M., Chang, Y.W., Holzbaur, E.L.F., and Jongens, T.A. (2024). FMRP regulates MFF translation to locally direct mitochondrial fission in neurons. Nat. Cell Biol. *26*, 2061–2074. https://doi.org/10.1038/S41556-024-01544-2.

44. Kataoka, K., Bilkei-Gorzo, A., Nozaki, C., Togo, A., Nakamura, K., Ohta, K., Zimmer, A., and Asahi, T. (2020). Age-dependent Alteration in Mitochondrial Dynamics and Autophagy in Hippocampal Neuron of Cannabinoid CB1 Receptor-deficient Mice. Brain Res. Bull. *160*, 40–49. https://doi.org/10.1016/J.BRAINRESBULL.2020.03.014.

45. Gratacós, F.M., and Brewer, G. (2010). The role of AUF1 in regulated mRNA decay. Wiley Interdiscip. Rev. RNA *1*, 457–473. https://doi.org/10.1002/WRNA.26.

46. Doxakis, E. (2014). RNA binding proteins: A common denominator of neuronal function and dysfunction. Neurosci. Bull. *30*, 610–626. https://doi.org/10.1007/S12264-014-1443-7.

47. Zhang, G., Neubert, T.A., and Jordan, B.A. (2012). RNA Binding Proteins Accumulate at the Postsynaptic Density with Synaptic Activity. J. Neurosci. *32*, 599–609. https://doi.org/10.1523/JNEUROSCI.2463-11.2012.

48. Jurado, S., Rodríguez-Pascual, F., Sánchez-Prieto, J., Reimunde, F.M., Lamas, S., and Torres, M. (2006). NMDA induces post-transcriptional regulation of α2-guanylyl-cyclase-subunit expression in cerebellar granule cells. J. Cell Sci. *119*, 1622–1631. https://doi.org/10.1242/JCS.02867.

49. Zalfa, F., Giorgi, M., Primerano, B., Moro, A., Di Penta, A., Reis, S., Oostra, B., and Bagni, C. (2003). The Fragile X Syndrome Protein FMRP Associates with BC1 RNA and Regulates the Translation of Specific mRNAs at Synapses. Cell *112*, 317–327. https://doi.org/10.1016/S0092-8674(03)00079-5.

50. Bassell, G.J., and Warren, S.T. (2008). Fragile X Syndrome: Loss of Local mRNA Regulation Alters Synaptic Development and Function. Neuron *60*, 201–214. https://doi.org/10.1016/j.neuron.2008.10.004.

51. Wang, Z., Qiao, D., Chen, H., Zhang, S., Zhang, B., Zhang, J., Hu, X., Wang, C., Cui, H., Wang, X., and Li, S. (2023). Effects of Fmr1 Gene Mutations on Sex Differences in Autism-Like Behavior and Dendritic Spine Development in Mice and Transcriptomic Studies. Neuroscience *534*, 16–28. https://doi.org/10.1016/j.neuroscience.2023.10.001.

52. Prashad, S., and Gopal, P.P. (2021). RNA-binding proteins in neurological development and disease. RNA Biol. *18*, 972–987. https://doi.org/10.1080/15476286.2020.1809186.

53. Korb, E., Herre, M., Zucker-Scharff, I., Gresack, J., Allis, C.D., and Darnell, R.B. (2017). Excess Translation of Epigenetic Regulators Contributes to Fragile X Syndrome and Is Alleviated by Brd4 Inhibition. Cell *170*, 1209–1223.e20. https://doi.org/10.1016/J.CELL.2017.07.033.

54. Quesnel-Vallières, M., Dargaei, Z., Irimia, M., Gonatopoulos-Pournatzis, T., Ip, J.Y., Wu, M., Sterne-Weiler, T., Nakagawa, S., Woodin, M.A., Blencowe, B.J., and Cordes, S.P. (2016). Misregulation of an Activity-Dependent Splicing Network as a Common Mechanism Underlying Autism Spectrum Disorders. Mol. Cell *64*, 1023–1034. https://doi.org/10.1016/j.molcel.2016.11.033.

55. Irimia, M., Weatheritt, R.J., Ellis, J.D., Parikshak, N.N., Gonatopoulos-Pournatzis, T., Babor, M., Quesnel-Vallières, M., Tapial, J., Raj, B., O'Hanlon, D., et al. (2014). A highly conserved program of neuronal microexons is misregulated in autistic brains. Cell *159*, 1511–1523. https://doi.org/10.1016/J.CELL.2014.11.035.

56. Innocenzi, E., Sciamanna, G., Zucchi, A., Medici, V., Cesari, E., Farini, D., Elliott, D.J., Sette, C., and Grimaldi, P. (2025). Modulation of Neurexins Alternative Splicing by Cannabinoid Receptors 1 (CB1) Signaling. Cells *14*, 972. https://doi.org/10.3390/CELLS14130972/S1.

57. Licznerski, P., Park, H.A., Rolyan, H., Chen, R., Mnatsakanyan, N., Miranda, P., Graham, M., Wu, J., Cruz-Reyes, N., Mehta, N., et al. (2020). ATP Synthase c-Subunit Leak Causes Aberrant Cellular Metabolism in Fragile X Syndrome. Cell *182*, 1170–1185.e9. https://doi.org/10.1016/J.CELL.2020.07.008.

58. Kajdasz, A., Niewiadomska, D., Sekrecki, M., and Sobczak, K. (2022). Distribution of alternative untranslated regions within the mRNA of the CELF1 splicing factor affects its expression. Sci. Rep. *12*, 190. https://doi.org/10.1038/s41598-021-03901-9.

59. Popovitchenko, T., Park, Y., Page, N.F., Luo, X., Krsnik, Z., Liu, Y., Salamon, I., Stephenson, J.D., Kraushar, M.L., Volk, N.L., et al. (2020). Translational derepression of Elavl4 isoforms at their alternative 5′ UTRs determines neuronal development. Nat. Commun. *11*, 1674. https://doi.org/10.1038/s41467-020-15412-8.

60. DeLigio, J.T., Lin, G., Chalfant, C.E., and Park, M.A. (2017). Splice variants of cytosolic polyadenylation element–binding protein 2 (CPEB2) differentially regulate pathways linked to cancer metastasis. J. Biol. Chem. *292*, 17909–17918. https://doi.org/10.1074/JBC.M117.810127.

61. Lu, W.H., Yeh, N.H., and Huang, Y.S. (2017). CPEB2 Activates GRASP1 mRNA Translation and Promotes AMPA Receptor Surface Expression, Long-Term Potentiation, and Memory. Cell Rep. *21*, 1783–1794. https://doi.org/10.1016/j.celrep.2017.10.073.

62. Lu, W.H., Chang, T.T., Chang, Y.M., Liu, Y.H., Lin, C.H., Suen, C.S., Hwang, M.J., and Huang, Y.S. (2024). CPEB2-activated axonal translation of VGLUT2 mRNA promotes glutamatergic transmission and presynaptic plasticity. J. Biomed. Sci. *31*, 69. https://doi.org/10.1186/S12929-024-01061-2.

63. Hwang, J.Y., Monday, H.R., Yan, J., Gompers, A., Buxbaum, A.R., Sawicka, K.J., Singer, R.H., Castillo, P.E., and Zukin, R.S. (2022). CPEB3-dependent increase in GluA2 subunits impairs excitatory transmission onto inhibitory interneurons in a mouse model of fragile X. Cell Rep. *39*, 110853. https://doi.org/10.1016/J.CELREP.2022.110853.

64. Vuong, C.K., Wei, W., Lee, J.A., Lin, C.H., Damianov, A., de la Torre-Ubieta, L., Halabi, R., Otis, K.O., Martin, K.C., O'Dell, T.J., and Black, D.L. (2018). Rbfox1 Regulates Synaptic Transmission through the Inhibitory Neuron-Specific vSNARE Vamp1. Neuron *98*, 127–141.e7. https://doi.org/10.1016/J.NEURON.2018.03.008.

65. Nelson, S.B., and Valakh, V. (2015). Excitatory/Inhibitory Balance and Circuit Homeostasis in Autism Spectrum Disorders. Neuron *87*, 684–698. https://doi.org/10.1016/J.NEURON.2015.07.033.

66. Christensen, R., Kristensen, P.K., Bartels, E.M., Bliddal, H., and Astrup, A. (2007). Efficacy and safety of the weight-loss drug rimonabant: a meta-analysis of randomised trials. Lancet *370*, 1706–1713. https://doi.org/10.1016/S0140-6736(07)61721-8.

67. Alamancos, G.P., Pagès, A., Trincado, J.L., Bellora, N., and Eyras, E. (2015). Leveraging transcript quantification for fast computation of alternative splicing profiles. RNA *21*, 1521–1531. https://doi.org/10.1261/RNA.051557.115.

68. Rychlik, W. (2007). OLIGO 7 Primer Analysis. Software, 35–59. https://doi.org/10.1007/978-1-59745-528-2_2/.

69. Ye, J., Coulouris, G., Zaretskaya, I., Cutcutache, I., Rozen, S., and Madden, T.L. (2012). Primer-BLAST: a tool to design target-specific primers for polymerase chain reaction. BMC Bioinf. *13*, 134. https://doi.org/10.1186/1471-2105-13-134.

70. Livak, K.J., and Schmittgen, T.D. (2001). Analysis of relative gene expression data using real-time quantitative PCR and the 2(-Delta Delta C(T)) Method. Methods *25*, 402–408. https://doi.org/10.1006/METH.2001.1262.

71. Kilkenny, C., Browne, W.J., Cuthill, I.C., Emerson, M., and Altman, D.G. (2010). Improving bioscience research reporting: The ARRIVE guidelines for reporting animal research. J. Pharmacol. Pharmacother. *1*, 94–99. https://doi.org/10.4103/0976-500X.72351.

72. Percie du Sert, N., Hurst, V., Ahluwalia, A., Alam, S., Avey, M.T., Baker, M., Browne, W.J., Clark, A., Cuthill, I.C., Dirnagl, U., et al. (2020). The ARRIVE guidelines 2.0: Updated guidelines for reporting animal research. PLoS Biol. *18*, e3000410. https://doi.org/10.1371/JOURNAL.PBIO.3000410.

73. Bergadà-Martínez, A., de los Reyes-Ramírez, L., Martínez-Torres, S., Ciaran-Alfano, L., Martínez-Gallego, I., Maldonado, R., Rodríguez-Moreno, A., and Ozaita, A. (2025). Sub-chronic administration of AM6545 enhances cognitive performance and induces hippocampal synaptic plasticity changes in naïve mice. Br. J. Pharmacol. *182*, 2914–2929. https://doi.org/10.1111/BPH.70015.

74. Patro, R., Duggal, G., Love, M.I., Irizarry, R.A., and Kingsford, C. (2017). Salmon provides fast and bias-aware quantification of transcript expression. Nat. Methods, 417–417419. https://doi.org/10.1038/nmeth.4197.

75. Soneson, C., Love, M.I., and Robinson, M.D. (2016). Differential analyses for RNA-seq: Transcript-level estimates improve gene-level inferences. F1000Res. *4*, 1521. https://doi.org/10.12688/F1000RESEARCH.7563.2.

76. Love, M.I., Huber, W., and Anders, S. (2014). Moderated estimation of fold change and dispersion for RNA-seq data with DESeq2. Genome Biol. *15*, 550. https://doi.org/10.1186/S13059-014-0550-8.

77. Koopmans, F., van Nierop, P., Andres-Alonso, M., Byrnes, A., Cijsouw, T., Coba, M.P., Cornelisse, L.N., Farrell, R.J., Goldschmidt, H.L., Howrigan, D.P., et al. (2019). SynGO: An Evidence-Based, Expert-Curated Knowledge Base for the Synapse. Neuron *103*, 217–234.e4. https://doi.org/10.1016/j.neuron.2019.05.002.

78. Yu, G., Wang, L.G., Han, Y., and He, Q.Y. (2012). ClusterProfiler: An R package for comparing biological themes among gene clusters. OMICS *16*, 284–287. https://doi.org/10.1089/OMI.2011.0118.

79. Trincado, J.L., Entizne, J.C., Hysenaj, G., Singh, B., Skalic, M., Elliott, D.J., and Eyras, E. (2018). SUPPA2: Fast, accurate, and uncertainty-aware differential splicing analysis across multiple conditions. Genome Biol. *19*, 40. https://doi.org/10.1186/S13059-018-1417-1.

80. Hanada, Y., Ishihara, N., Wang, L., Otera, H., Ishihara, T., Koshiba, T., Mihara, K., Ogawa, Y., and Nomura, M. (2020). MAVS is energized by Mff which senses mitochondrial metabolism via AMPK for acute antiviral immunity. Nat. Commun. *11*, 5711. https://doi.org/10.1038/S41467-020-19287-7.

81. Delacher, M., Barra, M.M., Herzig, Y., Eichelbaum, K., Rafiee, M.R., Richards, D.M., Träger, U., Hofer, A.C., Kazakov, A., Braband, K.L., et al. (2020). Quantitative Proteomics Identifies TCF1 as a Negative Regulator of Foxp3 Expression in Conventional T Cells. iScience *23*, 101127. https://doi.org/10.1016/J.ISCI.2020.101127.

82. Schmittgen, T.D., and Zakrajsek, B.A. (2000). Effect of experimental treatment on housekeeping gene expression: Validation by real-time, quantitative RT-PCR. J. Biochem. Biophys. Methods *46*, 69–81. https://doi.org/10.1016/S0165-022X(00)00129-9.

83. Ramírez-López, A., Pastor, A., de la Torre, R., La Porta, C., Ozaita, A., Cabañero, D., and Maldonado, R. (2021). Role of the endocannabinoid system in a mouse model of Fragile X undergoing neuropathic pain. Eur. J. Pain *25*, 1316–1328. https://doi.org/10.1002/EJP.1753.

STAR★METHODS

KEY RESOURCES TABLE

REAGENT or RESOURCE	SOURCE	IDENTIFIER
Chemicals, peptides, and recombinant proteins		
Rimonabant	Axon Medchem	158681-13-1
Critical commercial assays		
RNAeasy miniKit	QIAGEN	74104
SMARTer Ultra Low Input kit	Takara Bio/Clontech	634940
NEBnext Ultra Directional RNA library prep kit for Illumina	New Englands Biolabs	E7420
High-capacity cDNA Reverse Transcription kit	Applied Biosystems	4368814
SYBR Green I PCR Master Mix	Roche	04707516001
Deposited data		
Raw bulk and synaptoneurosomal hippocampal data	This paper	GEO: GSE284627
Raw WT and FX hippocampal synaptoneurosomes data	This paper	GEO: GSE285032
Experimental models: Organisms/strains		
Mouse: FVB.129P2-Pde6b+Tyrc-ch Fmr1tm1Cgr/J	The Jackson Laboratory	RRID:IMSR_JAX:004828
Oligonucleotides		
Ddx6 inclusion forward sequence: TGGCCTCGGTGGTAGGA	This paper	N/A
Ddx6 inclusion probe sequence: CGTGGGATTGAAGTGA	This paper	N/A
Ddx6 inclusion and exclusion reverse sequence: AGATATAATTCAAGCTTGTTAGAGGGC	This paper	N/A
Ddx6 exclusion forward sequence: GGAGCTTCGAGTCAACAATAAAGG	This paper	N/A
Ddx6 exclusion probe sequence: CGGTGATTGAAGTGAGTG	This paper	N/A
Celf1 inclusion forward sequence: GGCTGCGGAGGAGCAA	This paper	N/A
Celf1 inclusion probe sequence: CTGCTCAAAGAAAATGA	This paper	N/A
Celf1 inclusion reverse sequence: TATCAAGATGTTTGTGGGCCAG	This paper	N/A
Celf1 exclusion forward sequence: ATGGTGGATCATTGCTCTTTGA	This paper	N/A
Celf1 exclusion probe sequence: TTCCAGTCCTGTCTCAAA	This paper	N/A
Celf1 exclusion reverse sequence: AAAATGAACGGCACCCTGG	This paper	N/A
Cpeb2 inclusion forward sequence: CAGCCGGAACATCCAGAATAG	This paper	N/A
Cpeb2 inclusion probe sequence: CCAGGATCGAAGTAGAAT	This paper	N/A
Cpeb2 inclusion and exclusion reverse sequence: AGCTTGAATATGCACTCTCTGGAA	This paper	N/A
Cpeb2 exclusion forward sequence: GTTCAGGACAGACAACAATAGTAACACA	This paper	N/A
Cpeb2 exclusion probe sequence: TCTTACCCTTACAGGATCG	This paper	N/A
18S TaqMan gene expression assay	Applied Biosystems	Hs99999901_s1
Mff forward sequence: GGAGTTCCAAATGCCAGTGT	Hanada et al.[67]	N/A
Mff reverse sequence: TGGTGTTTTCAGTGCCAGAG	Hanada et al.[67]	N/A
Hnrnpd forward sequence: TGAAGTTGTAGACTGCACTCTG	Delacher et al.[68]	N/A
Hnrnpd forward sequence: CCAAAACCCCTTGATCGCC	Delacher et al.[68]	N/A
18S forward sequence: GTAACCCGTTGAACCCCATT	Schmittgen et al.[69]	N/A
18S forward sequence: CCATCCAATCGGTAGTAGCG	Schmittgen et al.[69]	N/A
B2m forward sequence: TTCTGGTGCTTGTCTCACTGA	Ramírez-López et al.[70]	N/A
B2m forward sequence: CAGTATGTTCGGCTTCCCATTC	Ramírez-López et al.[70]	N/A

(*Continued on next page*)

Continued

REAGENT or RESOURCE	SOURCE	IDENTIFIER
Software and algorithms		
Salmon v1.5.2	Patro et al.[66]	RRID: SCR_017036
Tximport v1.18	Soneson et al.[71]	RRID: SCR_016752
DESeq2 v1.30	Love et al.[72]	RRID: SCR_015687
SynGo	Koopmans et al.[73]	RRID: SCR_017330
Clusterprofiler v3.14	Yu et al.[74]	RRID: SCR_016884
SUPPA	Trincado et al.[75]; Alamancos et al.[76]	https://github.com/comprna/SUPPA
Primer Express	Applied Biosystems	RRID: SCR_014326
R v4.0	https://www.R-project.org/	RRID: SCR_001905
GraphPad Prism v10.0	GraphPad Software, Inc	RRID: SCR_002798

EXPERIMENTAL MODEL AND STUDY PARTICIPANT DETAILS

Fragile X mice in Friend Virus B (FVB.129) background (*Fmr1* KO, FVB.129P2-Pde6b+Tyrc-ch Fmr1tm1Cgr/J) and wild-type mice (WT, FVB.129P2-Pde6b+Tyrc-ch/AntJ) were purchased from The Jackson Laboratory and crossed to obtain FX and WT littermates used in this study. Young-adult male mice (8–15 weeks old) were randomly assigned to experimental groups and used for pharmacological approach. Mice were housed four per cage in a temperature (21 ± 1°C) and humidity (55 ± 10%) controlled environment with food and water available *ad libitum*. Pharmacological treatments were performed during the light phase of a 12 h cycle (lights on at 8 a.m.; light off at 8 p.m.). All animal procedures were performed following ''Animals in Research: Reporting Experiments'' (ARRIVE) guidelines in accordance with standard ethical guidelines[71,72] (European Directive 2010/63/EU) and were approved by the local ethical committee (Comitè Ètic d'Experimentació Animal-Parc de Recerca Biomèdica de Barcelona, CEEA-PRBB). In all experiments, only male mice were used. Sample size varies between n = 3–6 for *in silico* experiments and between n = 5–12 in molecular experiments.

METHOD DETAILS

Drugs

Rimonabant (0.1 mg/kg) from Axon Medchem was diluted in 5% ethanol, 5% cremophor-EL and 90% saline. Rimonabant and its vehicle were injected intraperitoneally (i.p.) during 7 days in a volume of 10 mL/kg of body weight.

Hippocampal bulk and synaptoneurosomal preparation from mouse brain

To obtain bulk and synaptoneurosomal hippocampal preparations from the same mouse, hippocampal tissues were rapidly dissected on ice, frozen on dry ice and stored at −80°C until used. Then, frozen hippocampal tissues were Dounce-homogenized by 10 strokes with a loose and 10 strokes with a tight pestle in 30 volumes of synaptoneurosome lysis buffer (in mM) (CaCl2 2.5, NaCl 124, KCl 3.2, K2H2PO4 1.06, NaHCO3 26, MgCl2 1.3, glucose 10, sacarose 0.32, HEPES/NaOH 20, pH 7.4) including phosphatase inhibitors (NaPyro 5, NaF 100, NaOrth 1, β-glycerolphospate 40) and protease inhibitors (leupeptin 1 mg/mL, aproptinin 10 μg/mL, pepstatin 1 μg/mL, phenylmethylsulfonyl fluoride 1 mM). Then, 35 μL of volume were collected and stored at −80°C as bulk hippocampal crude homogenate. The remaining volume was processed following synaptoneurosomal enrichment preparation.

Synaptoneurosomal enrichment preparation

Mouse hippocampal tissues were obtained 24 h after the last rimonabant (0.1 mg/kg, 7 days, i.p.) or vehicle administration and frozen at −80°C. Hippocampal tissues from all groups were processed in parallel to minimize variability following the protocol for synaptoneurosomal fractions previously described.[32,73] Specifically, the bulk homogenate or the remaining volume from bulk hippocampus preparation was centrifuged at 2,000×g for 1 min to recover the supernatant (S1) and the pellet was resuspended in 1 mL of synaptoneurosomes lysis buffer to further centrifuge at 2,000×g for 1 min. A second supernatant (S2) was recovered and combined with previous one (S1), and the combined supernatant (S1+S2) was filtered through a hydrophobic PTFE 10 μm filter (LCWP02500, Merck Millipore). The filtrate was centrifuged at 4,000×g for 1 min to attain the supernatant (S3) and then centrifuged at 14,000×g for 5 min, to obtain the pellet as the synaptoneurosomes.

RNA extraction

Hippocampal bulk and synaptoneurosome RNA were isolated using RNAeasy miniKit (74104, QIAGEN) following manufacturer's instructions.

RNA concentration, integrity and purity were measured using NanoDrop (Thermo Fisher Scientific) and Agilent 2100 Bioanalyzer (Agilent Technologies). RNA concentration and quality were uniform between samples and met the criteria of RIN >6.8.

RNA sequencing analysis

RNA libraries from hippocampal synaptoneurosomes and bulk hippocampus samples generated from the same animal were obtained by Macrogen Inc. using SMARTer Ultra Low Input kit (634940, Takara Bio/Clontech) according to manufacturer's instructions and sequenced using Illumina NovaSeq6000 flow cell. WT and FX hippocampal synaptoneurosomal samples treated with vehicle or rimonabant were processed at the Universitat Pompeu Fabra Genomics Facility. RNA libraries were generated using NEBnext Ultra Directional RNA library prep kit for Illumina (E7420, New Englands Biolabs) following the manufacturer's protocols in combination with Poly(A) mRNA magnetic isolation module (NEB) and were sequenced using Illumina NextSeq500 high-throughput flow cell. Raw data were deposited on the Gene Expression Omnibus (GEO) database and made publicly available with the identifier GEO:GSE284627, for bulk and synaptnoneurosomal hippocampus, and GEO:GSE285032, for WT and FX hippocampal synaptoneurosomes.

Pseudogenes were removed from Ensembl GRCm39 annotation to further obtain transcript abundance in transcripts per million (TPM) using *Salmon* 1.5.2[74] in its quasi-mapping based mode. Gene and transcript level quantification in counts per million (CPM) were obtained from TPMs using *tximport* (v1.18) R package.[75]

Differential expression analysis

Low-level expressed genes and transcripts were filtered out based on mean CPM >1 in at least one of the experimental conditions. Differential expression analyses at gene and transcript level were performed using *DESeq2* (v1.30) Bioconductor package.[76] Four comparisons were made: synaptoneurosome transcriptome (bulk hippocampus vs. synaptoneurosomes, HC-BULK vs. HC-SYN), genotype effect (WT-VEH vs. FX-VEH), treatment effect in FX mice (FX-VEH vs. FX-RIM) and rimonabant effect in WT mice (WT-VEH vs. WT-RIM).

Differential expression was estimated based on fold-changes, and *p*-values were corrected using the Wald test procedure, with a significance cut-off set as $|\log_2 FC| > 0.2$ and adjusted $p < 0.1$ for differential gene expression (DGE) analysis and adjusted $p < 0.05$ for differential transcript expression (DTE) analysis. Overrepresentation enrichment analyses were performed to investigate synaptoneurosomes composition with *SynGO*[77] against brain expressed background, setting medium stringency and top and second level terms as labels for cellular component analysis. Enrichment analysis for the genes associated with differentially expressed transcripts was performed with *clusterProfiler* (v3.14) Bioconductor package.[78] Each differentially expressed gene set was analyzed separately using all synaptoneurosomes expressed genes as background. Benjamini-Hochberg multiple testing was used to calculate the *p*-value and results were determined statistically significant at an adjusted $p < 0.05$ for each gene ontology (GO) term.

Alternative splicing analysis

AS analysis was performed using *SUPPA*[67,79] to predict the relative inclusion and differential splicing of skipping exon (SE), alternative first and last exon (AF and AL), alternative 5′ and 3′ splice-site (A5 and A3), mutually exclusive exons (MX), and retained intron (RI) (Figure S2A). The relative inclusion of each event for all experimental groups was calculated as Percent Spliced In (PSI) using TPM previously obtained, with a minimum of 1 TPM expression of the transcripts involved in the event. To test differential inclusion in each comparison, delta PSI (dPSI) was calculated, using the empirical method, as the difference of the mean PSI from each group: genotype effect ($PSI_{FX\text{-}VEH} - PSI_{WT\text{-}VEH}$), treatment effect in FX ($PSI_{FX\text{-}RIM} - PSI_{FX\text{-}VEH}$) and rimonabant effect in WT ($PSI_{WT\text{-}RIM} - PSI_{WT\text{-}VEH}$). The significance of each event was calculated using a linear regression model and *p*-values were corrected by gene using the false discovery rate (*FDR*). An event was considered significant when $|dPSI| > 0.05$ and adjusted $FDR < 0.05$.

Cell-type specificity enrichment analysis

Cell-type distribution of genes harboring AS events was performed by cross-referencing our target genes with a reference murine hippocampal single-cell transcriptomic dataset.[23] Genes not found in the reference dataset or with zero expression in all cellular populations were excluded from the analysis. For each identified gene, we retrieved the relative expression (expressed in percentages) across five primary brain cell populations: neurons, astrocytes, microglia, oligodendrocytes and vascular cells. For representation purposes, we aggregated the expression of all non-neuronal populations into glia and vascular fraction, and we highlighted the main cell type classification based on the individual population with the highest relative expression percentage.

Specific assays for alternative splicing events

To detect complete AS events, we designed custom TaqMan gene expression assays (4331348, Applied Biosystems) for the inclusion and the exclusion of each event (Figure S2B). Thus, each assay allows the detection of the transcripts that cover both, the exon inclusion and the exon exclusion. Primers and internal probes for inclusion/exclusion were designed using Primer Express (4363991, Applied Biosystems) software. Primer dimerization and specificity were checked with OLIGO[68] and PrimerBLAST[69] tools.

Gene expression and alternative splicing analysis by qRT-PCR

Comparable amounts of RNA from hippocampal synaptoneurosomes and bulk hippocampus were reverse transcribed to cDNA using the High-capacity cDNA Reverse Transcription kit (4368814, Applied Biosystems) following the manufacturer's instructions and stored at −20°C until use. Quantitative real-time PCR (qRT-PCR) was carried out in triplicate with QuantStudio 12K Flex Real-Time PCR System (4471134, Applied Biosystems). Quantification was performed using the comparative double-delta Ct method[70] and the fold change was calculated using the equation $2^{-\Delta\Delta Ct}$.

For gene expression, qRT-PCR using SYBR Green I PCR Master Mix (04707516001, Roche) was performed in 10 μL reaction using 0.1 ng/μL of cDNA. Previously described primers were used for both bulk hippocampus and hippocampal synaptoneurosomes quantification of *Mff* (F: 5′-GGAGTTCCAAATGCCAGTGT-3′ and R: 5′-TGGTGTTTTCAGTGCCAGAG-3′)[80] and *Hnrnpd* (F: 5′-GTGAAGT TGTAGACTGCACTCTG-3′ and R: 5′-CCAAAACCCCTTGATCGCC-3′).[81] Each gene was normalized using *18S* (F: 5′-GTAACCCGTT GAACCCCATT-3′ and R: 5′-CCATCCAATCGGTAGTAGCG-3′)[82] or *B2m* (F: 5′-TTCTGGTGCTTGTCTCACTGA-3′ and R: 5′-CAGTA TGTTCGGCTTCCCATTC-3′)[83] as endogenous control for hippocampal synaptoneurosomes and bulk hippocampus samples, respectively.

For inclusion and exclusion AS events expression, qRT-PCR using TaqMan chemistry (4369016, Applied Biosystems) was performed in 5 μL reaction using 0.08 ng/μL of hippocampal synaptoneurosomal cDNA or 0.1 ng/ul of bulk hippocampal cDNA. Customized TaqMan probes (Figure S7) were used to detect each splicing event and probe for *18S* (Hs99999901_s1) was used as endogenous control for events normalization.

To estimate the relative gene and inclusion/exclusion expression, control sample (WT-VEH) was standardized at a value of 1. To estimate each AS event expression, an experimental differential Percent Spliced In (experimental dPSI) was calculated, similarly as *SUPPA* did. First, experimental PSI (ePSI) was calculated as 2^{-Ct} expression levels of inclusion divided by the sum of inclusion and exclusion 2^{-Ct} expression levels for each AS event. Then, experimental dPSI was calculated as the difference of the mean ePSI from each group: genotype effect ($ePSI_{FX\text{-}VEH} - ePSI_{WT\text{-}VEH}$) and treatment effect in FX ($ePSI_{FX\text{-}RIM} - ePSI_{FX\text{-}VEH}$).

QUANTIFICATION AND STATISTICAL ANALYSIS

Data was analyzed with RStudio (v4.0) and GraphPad Prism (v10.0) software. Statistical details of each experiment can be found in the figures legends and results. The exact sample size can be found in figure legend, being between 3 and 6 for *in silico* experiments and between 5 and 12 for molecular experiments. *In silico* results were reported as unique fold-change or PSI value being each dot the change in each comparison. Significance in differential expression analyses were estimated using the Wald test and in AS analyses using the FDR. Molecular results were reported as mean ± standard error of the mean (s.e.m), being each dot the measure of an independent animal. Statistical comparisons were evaluated using unpaired Student's *t* test (two groups comparisons) or one-way ANOVA (multiple comparisons). Subsequent Tukey's *post hoc* test analysis was used when required (significant interaction between factors). Comparisons were considered statistically significant when $p < 0.05$ and indicated in figure legends.